Electronic Supplementary Material (ESI) for ChemComm.

The Same but Different: Multiple Functions of the Fungal Flavin Dependent Monooxygenase SorD from *Penicillium chrysogenum*

Lukas Kahlert [a], Russell J. Cox [a] and Elizabeth Skellam [a,*]

Supporting Information

Table of Contents

General information

Reagents

Analytical grade chemicals, reagents and solvents were purchased from Sigma Aldrich, Roth and Fischer. Molecular biology procedures were performed according to general standards and molecular biology kits were used according to the manufacturer's protocols. Analytical PCR was performed using OneTaq polymerase and preparative PCR for cloning procedures was performed using Q5 polymerase, both manufactured by NEB. Restriction endonucleases were purchased from NEB.

Media

All media were prepared using deionised water and autoclaved at 126 °C for 20 min. See Table S1 for details.

Analytical LCMS

LCMS data were obtained with a Waters 2767 sample manager connected to Waters 2545 pump and System Fluidics Organizer (SFO), a Phenomenex Kinetex column (2.6µ,C18, 100 Å, 4.6 × 100 mm) equipped with a Phenomenex Security Guard precolumn (Luna C5 300 Å) eluted at 1.0 mL min^{-1}, with a waters 2998 Diode Array detector (210–600 nm) and Waters 2424 ELSD and Waters SQD-2 mass detector operating simultaneously in ES^+ and ES^- modes between 100 and 1000 *m/z*. Solvents were: A, HPLC-grade H_2O containing 0.05% formic acid and B, HPLC-grade acetonitrile containing 0.045% formic acid. The gradient was run over 15 min starting at 10 % B and ramping to 90 % B within the first ten minutes, followed by two minutes at 90 % B and returning to 10 % B over the final three minutes.

Preparative LCMS

Purification of compounds was achieved using a Waters mass-directed autopurification system comprising of a Waters 2767 autosampler, Waters 2545 pump system, a Phenomenex Kinetex Axia column (5µ, C18, 100 Å, 21.2 × 250 mm) equipped with a Phenomenex Security Guard pre- column (Luna C5 300 Å) eluted at 20 mL min^{-1} at ambient temperature. Solvents were used as above. The post-column flow was split (100:1) and the minority flow was made up with HPLC-grade MeOH + 0.045% formic acid to 1 mL min^{-1} for simultaneous analysis by diode array (Waters 2998), evaporative light-scattering (Waters 2424) and electrospray ionisation mass spectrometry in positive and negative modes (Waters SQD-2). Detected peaks were collected into glass tubes. Combined fractions were evaporated with a vacuum centrifuge, weighed, and residues dissolved directly in deuterated solvent for NMR.

HRMS and NMR

HRMS was obtained using a Waters Acquity Ultraperformance UPLC system connected to a Q-TOF Premier mass spectrometer. NMR data were recorded using a Bruker Ascend 600 instrument equipped with a cryo-cooled probe at 600 MHz (^1H) and 125 MHz (^{13}C) and are referenced relative to Me_4Si. 2D spectra (1^H-1^HCOSY, HSQC and HMBC) were recorded using standard parameters. Samples were dissolved in deuterated solvents as indicated in the respective NMR tables and figures.

Experimental Procedures

Fermentation and Extraction Protocols

A spore suspension of *Aspergillus oryzae* transformants grown on selective agar plates (CZD/S1 or CZD/S1 w/o methionine) was inoculated into 100 mL DPY-medium in a 500 mL baffled flask and incubated for four days at 28 °C with 110 rpm shaking. Cultures were homogenized using a hand blender and cells were separated by filtration. The liquid supernatant was acidified with 2 M HCl to pH 3-4 and extracted twice with ethyl acetate (2 x 100 mL). Organic layers were combined, dried over $MgSO_4$ and solvent was removed under reduced pressure. The organic residue was dissolved in methanol to a concentration of 10 mg/mL, filtered over glass wool and analysed by LCMS (analytical). For preparative LCMS cultures were grown on a 1.5 L scale and the concentration of the organic extract applied for purification was 40 mg/mL.

Construction of *A. oryzae* Expression Vectors

Expression vectors were constructed as described in our previous paper.[1] A synthetic pMA-T plasmid harbouring intron-free *sorD* (*P. chrysogenum*) was purchased at Thermo Fischer and used as template for amplification of *sorD* (*P. chrysogenum*). All primers and vectors constructed during this work are listed in Table S2 and S3, respectively.

Transformation of *A. oryzae* NSAR1

A. oryzae NSAR1 was grown on DPY agar (approximately 1 week), spores were suspended in ddH_2O and used to inoculate 50 mL (250 mL flask) of GN liquid culture which was incubated for ca. 16 h (28 °C, 110 rpm). Cells were collected by filtration over sterile miracloth, washed with 0.8M NaCl and suspended in 10 mL of filter-sterilised *A. oryzae* NSAR1 protoplasting solution (10 mg/mL lysing enzyme from *Trichoderma harzianum*, Sigma-Aldrich, 0.8M NaCl). The suspension was incubated for 4 h at ambient temperature with gentle shaking. Protoplasts were released from hyphal strands by pipetting, collected by centrifugation (3.000 g, 5 min) and directly suspended in the required amount of fungal transformation solution I (10mM $CaCl_2$, 0.8M NaCl and 50mM Tris-HCl at pH 7.5). Vector DNA (≥1 µg in 10 µL of ddH_2O) was mixed with 100 µL protoplasts and incubated on ice for 2 min. 1 mL of fungal transformation solution II (10mM $CaCl_2$, 0.8M NaCl and 50 mM Tris-HCl at pH 7.5, 60% (*w/v*) PEG3350) was added and incubation proceeded at ambient temperature for another 20 min. 5 mL of molten selective soft agar (CZD/S1 or CZD/S1 w/o methionine) was added, the mixture was inverted and poured over selective agar plates (CZD/S1 or CZD/S1 w/o methionine). Plates were incubated at 28 °C until colonies appeared (4-6 days), which were transferred to secondary selection plates. Vividly growing colonies were transferred onto a third plate selective plate. Fungal strains used during this work are listed in Table S4.

Cloning, Expression and Purification of SorD (*P. chrysogenum*)

For expression of *sorD* (*P. chrysogenum*) in *E. coli* BL21 (DE3) the expression plasmid pET-28/a-*sorD* (encoding for an N-terminal hexa-histidine tag) was built by restriction digest with *Nde*I and *Not*I, followed by ligation using T4 ligase. pMA-T-*sorD* was used as template. Transformation of competent cells was performed based on a standard heat shock protocol. A pre-culture was grown overnight in LB-medium containing 50 µg/ mL kanamycin at 37 °C with 200 rpm shaking. Each 1 mL of this seed culture was used to inoculate 100 mL 2TY-medium containing 50 µg/ mL kanamycin. Cells were grown at 37 °C and 200 rpm until an OD_{600} between 0.4-0.6 was reached. Protein expression was induced by addition of Isopropyl-β-D-thiogalactopyranoside (IPTG) to a final concentration between 0.1 mM and 0.7 mM and cells were incubated for another 16 h at 16 °C and 200 rpm. Cells were harvested by centrifugation (3500 g, 10 min) at 4 °C, resuspended in loading buffer (50 mM Tris-HCL pH 8.0, 150 mM NaCl, 10 mM imidazole, 10% glycerol (*v/v*)) and lysed by sonication. Cell debris was removed from the total lysate by centrifugation (10.000 g, 40 min, 4 °C). Protein production was assessed by SDS-PAGE where SorD (52 kDa)

was only present in the insoluble fraction (Figure S3). Lowering the expression temperature to 12°C yielded only insoluble protein as well. The procedure was repeated using a construct where the first 23 amino acid residues of the protein were excluded (putative N-terminal signal sequence), but again resulted only in insoluble protein (50 kDa; Figure S4). Using LB- or TB-media also yielded solely insoluble protein. The alternate expression strain *E. coli* Arctic Express (DE3) was transformed with pET18/a harbouring the truncated *sorD* and a pre-culture was prepared as described beforehand (with additional 20µg/mL gentamycin). 2mL of this seed culture were used to inoculate 100 mL LB containing no antibiotics. Cells were grown at 30 °C and 200 rpm for 3h. Protein expression was induced by addition of IPTG to a final concentration of 0.1 mM and cells were incubated for another 16 h at 12 °C and 200 rpm. Harvesting was performed as described above, but SorD remained insoluble (Figure S5A). The strain *E. coli* BL21 (DE3) expressing the full *sorD* was alternatively cultivated in LBE-5052 medium (50 µg/ mL kanamycin, 37°C until OD_{600}between 0.4-0.6 then 44h at 16°C) for autoinduction of protein expression, but no soluble target protein was detected by SDS-PAGE (Figure S5 B).

Feeding experiments

5a: *A. oryzae* NSAR1 (control) and *A. oryzae* expressing Pc*sorD* were grown in DPY medium at 28°C with and shaking for 3 days. 3mg of epoxysorbicillinol **5a** dissolved in 300 µL DMSO were added to each culture and incubation was continued for 20 hours. Extraction and analysis were performed as described above.

2ab: *A. oryzae* NSAR1 (control) and *A. oryzae* expressing *PcSrD* were grown in DPY medium at 28°C with and shaking for 3 days. Substrate **2ab** was prepared by incubating **1ab** with purified SorC for one hour as described previously.[1] Approx. 1mg of **2ab** mixture were added to each culture and incubation was continued for 20 hours. Extraction and analysis were performed as described above.

Whole Cell Extract and Cell Free Extract assays with PcSorD

Preparation: *A. oryzae* expressing *sorD* (*P. chrysogenum*) was grown in DPY medium at 28°C with and shaking for 3 days. Cells were collected by Büchner filtration and broken up one using of the following methods: Dry cells were frozen in liquid nitrogen and ground using mortar and pestle. Ground cells were resuspended in 50 mM phosphate buffer (pH 8). This mixture was either used directly for assays (Whole Cell Extract; WCE) or cell debris were removed by filtration (Cell Free Extract; CFE). Alternatively, WCE and CFE were prepared by resuspending dry cells in 50 mM phosphate buffer (pH 8) and cells broken using a hand blender.

Assays: 200 µL of WCE and CFE were separately supplemented with a mixture of NADH/NADPH and epoxysorbicillinol **5a** dissolved in acetone (total acetone in assay mixture ≤ 3 % v/v) and incubated at 28°C with shaking for 3 hours. Samples were extracted with 1 mL ethyl acetate and dried under vacuum. Organic residue was dissolved in 160 µL MeOH and subjected to LCMS analysis.

Biosynthetic Gene Cluster Analysis

Cluster identification: Draft genome of *T. reesei* QM6a was obtained from NCBI (WGS: AAIL02) and putative gene clusters were predicted using the secondary metabolites analysis tool fungiSMASH.[2] Among the 32 predicted gene clusters, the first shared 71 % homology with the sorbicillinoid biosynthetic gene cluster of *P. chrysogenum*. The respective cluster sequence was used as the query sequence for gene identification/ protein prediction with FGENESH.[3] Subsequently conserved domain analysis was performed using BLASTp. In same manner the sorbicillinoid biosynthetic gene cluster was identified in the draft genome of *P. chrysogenum* (WGS: JMSF01).

Accession numbers of SorD:

T. reesei QM6a: XP_006961562

P. chrysogenum: XP_002567557

ARTEMIS analysis: The alignment tool tBLASTx was used to create a comparison file between the sorbicillinoid BGC of *T. reesei* and *P. chrysogenum*. This file was used for identification of homologous proteins between the two cluster using ARTEMIS.[4] Results show that the following proteins are homologous: SorA, SorB, SorC, one MFS and one TF, but not SorD.

Phyre2 analysis: The protein fold recognition server Phyre2 was used for structural comparison of both SorD.[5] While both proteins have a predicted transmembrane helix comprised of 15 amino acid residues, the templates provided for both SorD are not matching. The best template for SorD from *T. reesei* is a vanillyl alcohol oxidase-type (VAO) FMO from the thermophilic fungus *Myceliophthora thermophila* (PDB 6F73) with no identified substrate molecules.[6] The best template for SorD from *P. chrysogenum* is a xylooligosaccharide-specific oxidase, interestingly also from *Myceliophthora thermophila* and belonging to the VAO-type family as well (PDB 5K8E).[7]

Coding sequence of *sorD* from *T. reesei* QM6a

ATGTACGCCCCCCCTTTTGTCCGCGCCTTCGGAATCGCAGTCCTTGCCGTCCTCCCATCTTTCTCTTCGCCCGCAACTGCCGCTTCTCTGAAATCGTCCGGATCTTCGTCATCGTGCAG
ATGCTTCCCGGGAGACGCCTGCTGGCCATCCCCGGCCGACTGGAAGGCCTTCAACCAGTCCGTCGGCGGACGTCTCATTGCCACGGTCCCGCTTGGATCCGTCTGCCATGGCACC
ACGTATGATGCCGCACGCTGCGCAGACGTCAAAGCCGCATGGCCGTATGCGGACACACACACCGACTCGTCTAGTTCCGTCCTTGCGCCTTTCTTTGCGAACCAGAGCTGCGATCC
GTTTCTCCCTAGAGAGACTCCCTGCGTTATCGGCACATATGTCCAGTACGCCGTCAACGTCTCCAGCGTTGCAGACATCCAAAAGACTCTTGCGTTTTCTCAGAAGAAGAATCTTCG
CCTGGTAGTGAGAAACACGGGCCATGATTACTTTGGAAAGTCCACTGGAGCCGGTGGTCTGGGACTATGGATGCATAATCTCAAGACTTACGATATCCACGACTACAAGTCGGCT
GCTTACACTGGAAAAGCGGTCACCATGGGCGCGGGCATCCAGGCGGGAGAGTCTGCTGCTACTGCTTTCAAGCAAGGCCTTACCATTGTGTCTGGGATATGTCCGACTGTTGGCC
TGGCCGGAGGATACACCCAGGGCGGCGGCTTAGGGCCCTTGACGACCAGATACGGTCTCGGAGCTGACCAGGTACTGGAGTGGCATGCGGTGCTTGCAAACGGCTCCGAAATC
ACTGCGACTCCAACCAAGAACAGCGATCTGTACTGGGCCTTGACTGGTGGCGGTGGTGGCACATACGCCGTCGTGTACTCCATGACCGTCAAAGCACATGCAAACGAGAAGACC
ACAGGGGCGAATCTCACGTTTCCGAATGCCGGGTCAGAAGATGTCTTCTTTCAGGGAGTTCAAGCATTTCACGATATTATACCTGCGATATCTGATGCCGGGGGCACGGCGGTCT
GGACCGTGCTTTCCAAGGCCTTGTCCGTTGGGCCAGTTACCGGGCCGAACATGACCAAGGCGACCATGGATAGCATCTTTCAGCCCGTGCTCCAGAAACTGGATGCTCTCAATATT
ACATACTCCTACTCCTCTGGGGAGTTTTCAAGCTTTTATGAGAGCAACGCCGCTTATGACCCACCGGTGGTGTCAAATGGTCTCCAAATTGGCGGCAGACTCGTAAAGCGGTCTGA
CTTTACCGGGAACCCAGACGGCTTCATCCAGGCCATTCGTGGTATCGCCGATCAAGGTGGACTGGTCACCGGGGCCTCATACCAGCTATCGAGCAGCCTCCAACACCCGCCCAACT
CGGTGAACCCAGAGCTGAGGAAGAGCTTGATTTCGTTTCAGATCGGAGTACCCTGGATCAACACAGACTGGGCTACAGATCTTCACAACCAGGATCTCATCACCAACTCATTCGTA
CCCGCGCTGGCTGCCCTTCTTCCCAGTGGGGGCTCTGCTTACCTTAACCAGGCGGACTTCCGGGAACCAGGATGGCAGCAGGTATTTTACGGAGAAAACTATGAGAAACTGCTTG
AGTTGAAGGATGTGTATGACCCTAATGGGGTCTTCTGGGGAAGGACTACGGTTGGGAGCGAACGGTGGGCTGAGACGGAAGATAAGCGCCTTTGCCGAGTCTCGTAA

Sequence of SorD from *T. reesei* QM6a (residues putatively involved in covalent binding of FAD are highlighted in red)

MYAPPFVRAFGIAVLAVLPSFSSPATAASLKSSGSSSSCRCFPGDACWPSPADWKAFNQSVGGRLIATVPLGSVCHGTTYDAARCADVKAAWPYADTHTDSSSSVLAPFFANQSCDPFLP
RETPCVIGTYVQYAVNVSSVADIQKTLAFSQKKNLRLVVRNTG**H**DYFGKSTGAGGLGLWMHNLKTYDIHDYKSAAYTGKAVTMGAGIQAGESAATAFKQGLTIVSGI**C**PTVGLAGGYTQ
GGGLGPLTTRYGLGADQVLEWHAVLANGSEITATPTKNSDLYWALTGGGGGTYAVVYSMTVKAHANEKTTGANLTFPNAGSEDVFFQGVQAFHDIIPAISDAGGTAVWTVLSKALSVG
PVTGPNMTKATMDSIFQPVLQKLDALNITYSYSSGEFSSFYESNAAYDPPVVSNGLQIGGRLVKRSDFTGNPDGFIQAIRGIADQGGLVTGASYQLSSSLQHPPNSVNPELRKSLISFQIGVP
WINTDWATDLHNQDLITNSFVPALAALLPSGGSAYLNQADFREPGWQQVFYGENYEKLLELKDVYDPNGVFWGRTTVGSERWAETEDKRLCRVS

Coding sequence of *sorD* from *P. chrysogenum*

ATGCAGGCCGCCAGTGCATTTGCGACCTGTCTCTTGGCTTCAGTGGGTGGCAACAGCAGCGCCGTCGCCTTTCCAAACCAAGCCAACTATTCTACTCTTGTCGCGCCGTACAATTTC
GATCTTCTCACCACCCCTTCCGCCATTGTCTGGCCCCAGGATACACAGCAGGTAGCAGCCGCCGTCAAATGTGCCGTGGATTCAGACATCAAAGTTCAACCGAAAAGCGGCGGAC
ACAACTATGGCAACTATGGATCAACCACCGGCGAGCTGTCTGTGAATCTGGACAATCTGCAGCACTTCAGCATGGATGAAACCAGCTGGACTGCCAGATTGGGACCAGGTAACCG
CCTAGGCCGAGTCACCGAGCTCATGTATAACAACGGTGGTCGACATGTTCCACATGGGACGACCTTCACGGTGGGACTCGGTGGACACGCAACTGTTGGAGGTGCCGGAGCGGC
ATCACGAATGCACGGACTGTTGCTCGACTATGTGGAGGAGGTAGAGGTTGTTCTGGCCAACTCATCCATCGTCCGAGCATCCAAGTCTCACAACGAGGATCTTTTCTTCGCCGTGC
GTGGTGCCGCTTCAAGCGTTGGCATTGTGACCGACTTTTCTATACGCACCGAGCCCGTTCCCGTATCCAGCGTCACTTACTCTTATATCTGGGAGGGGACAGATCCAGCAGCCCGC
GCAGAAGTATTCTTGACTTGGCAGTCATTGCTCGCCGGTGGCTCTTTGCCCCAACACATGGCCTACGATCTGGTTGCGACGGCGAATAGCATGATACTGGGTGGGGCTTACTTTGG
CAGTCAGGAGGACTTCGAGGCCTTTAACCTCAGCAGCCACTTCAAAGTAGCGCCAGACGTCGCACATATAAAAACATATACCAACTTCTTCGACTTCTCCGCCGCCGCAAGCGCTC
AGACTAAAGCAGCTGGGATTGCTTCCCCGTCGCATTTCTATGCCAAATCTCTCGTCTTCAATCAACAGACTCTCATACCTGATGATGCTGCTGAGGAGGTCTTCAAGTACTTGGCCA
CGACCAAGAATGGTACTGATTTGTACGCGGTCACTTTCGCCGCATTGGGTGGTGCGGTGAGGGACGTCTCGGCATCAGAAACAGCTTTCTATCACCGTGATGCTTCATACTTTATG
TTCTCCTTTGGAAGGACTAGTGGAGACCTGACTGACACGACGGTGCAGTTCCTGGATGGGCTGAGCGAAGTTCTGACTAGTGGGCAACCCGATGCCTACTACGGCCAGTACGTG
GGGAATGTCGATCCCAGACAATCAACTGACAAGGCATTGACGGGGTATTATGGCAAGAATCTGCATCGCCTGCAGCAGATCAAGTCTGCGGTAGACCCGAATGATGTTTTCCATA
ACCAGCAGAGTATCCCACCTCTGTCCTAG

Sequence of SorD from *P. chrysogenum* (residues putatively involved in covalent binding of FAD are highlighted in red)

MQAASAFATCLLASVGGNSSAVAFPNQANYSTLVAPYNFDLLTTPSAIVWPQDTQQVAAAVKCAVDSDIKVQPKSGG**H**NYGNYGSTTGELSVNLDNLQHFSMDETSWTARLGPGNRL
GRVTELMYNNGGRHVPHGTTFTVGLGGHATVGGAGAASRMHGLLLDYVEEVEVVLANSSIVRASKSHNEDLFFAVRGAASSVGIVTDFSIRTEPVPVSSVTYSYIWEGTDPAARAEVFLT
WQSLLAGGSLPQHMAYDLVATANSMILGGAYFGSQEDFEAFNLSSHFKVAPDVAHIKTYTNFFDFSAAASAQTKAAGIASPSHFYAKSLVFNQQTLIPDDAAEEVFKYLATTKNGTDLYA
VTFAALGGAVRDVSASETAFYHRDASYFMFSFGRTSGDLTDTTVQFLDGLSEVLTSGQPDAYYGQYVGNVDPRQSTDKALTGYYGKNLHRLQQIKSAVDPNDVFHNQQSIPPLS

Additional Figures and Tables

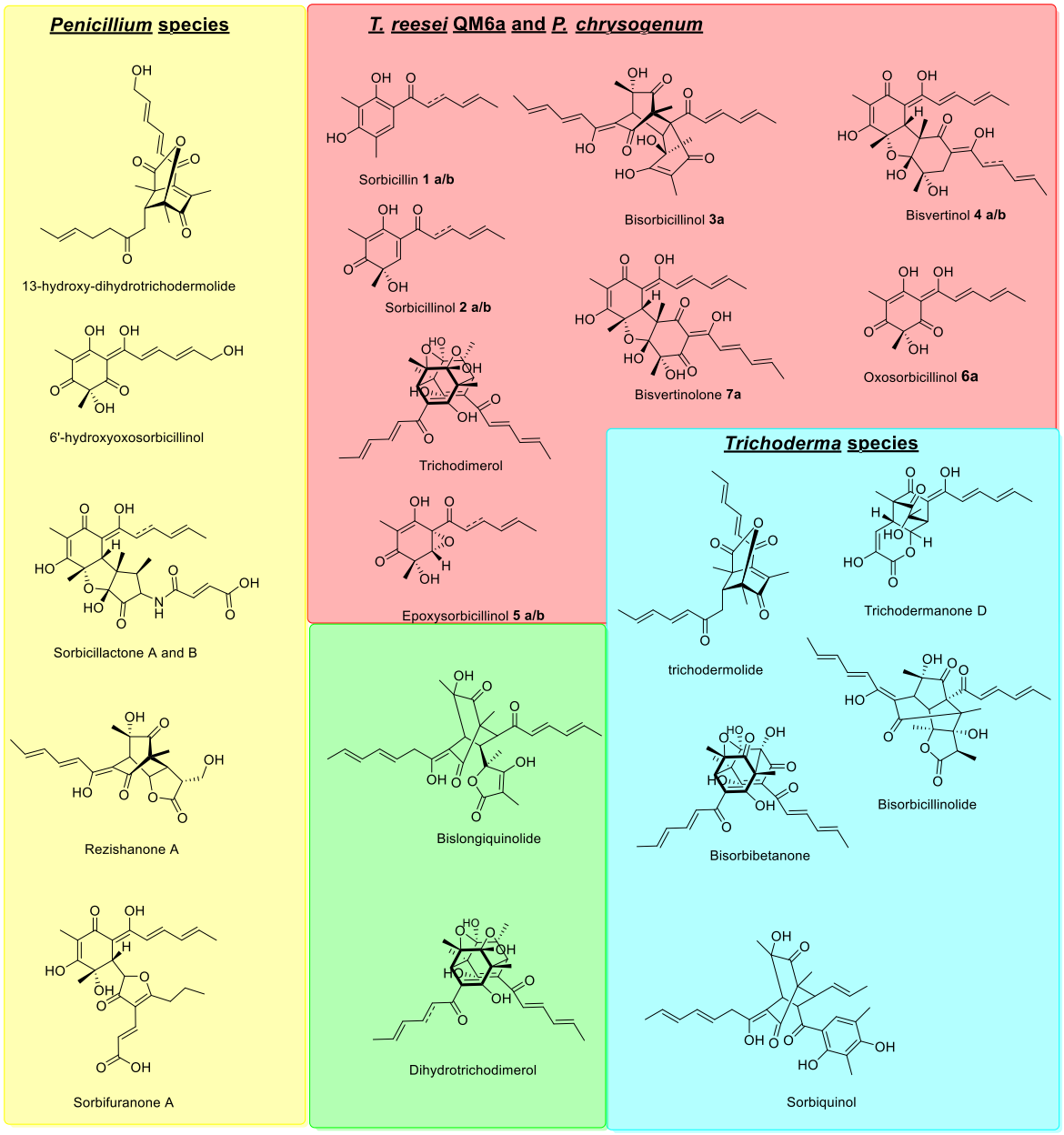

Figure S1: Overview of some (dimeric) sorbicillinoids produced by different species of *Trichoderma* and *Penicillium*. Color code: red, sorbicillinoids produced by both *T. reesei QM6a* and *P. chrysogenum;* yellow, sorbicillinoids only produced by *Penicillium* species; blue, sorbicillinoids only produced by *Trichoderma* species; green, sorbicillinoids produced by both *Trichoderma* and *Penicillium* species. See references for further details.[1,8–25] Compounds **6** and **7** have been shown to be derived from SorD in *P. chrysogenum* during this study.

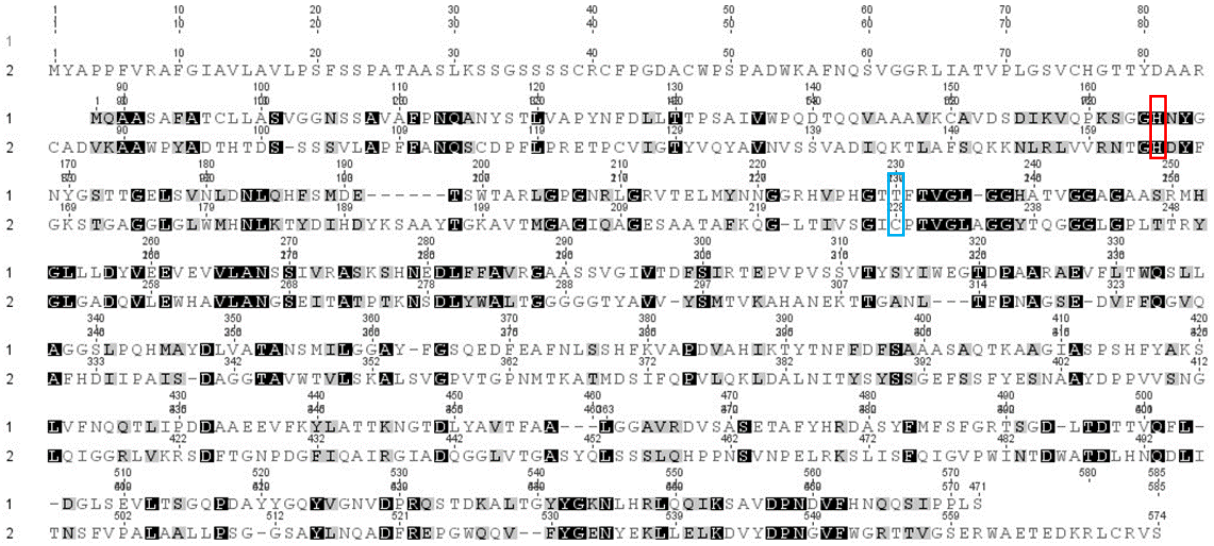

Figure S1: Geneious-alignment of PcSorD (sequence 1) and TrSorD (sequence 2). Parameters: Global alignment (Blosum62) with free end gaps, gap open penalty 12, gap extension penalty 3. Color code: black: identical, grey: similar, white: not similar. The histidine residue conserved in both FMO is highlighted with a red box and appears in a homologous region; the cysteine residue present in only TrSorD is highlighted in a blue box and appears in a region with no sequence similarity.

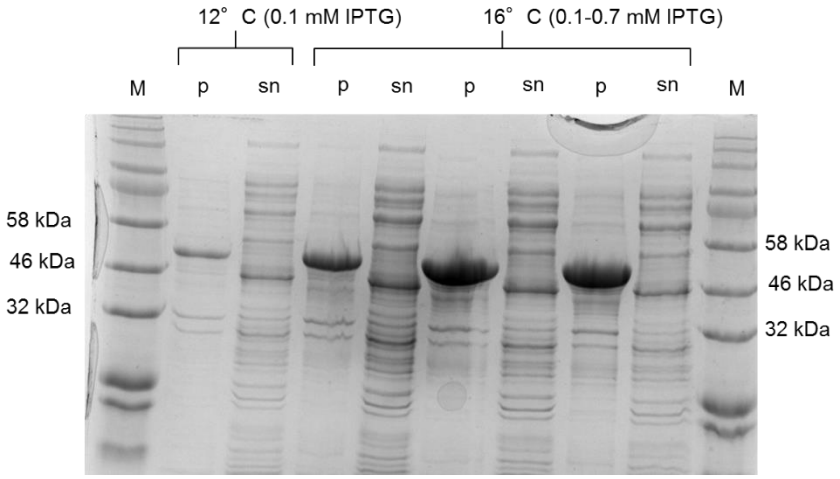

Figure S3: SDS-PAGE of SorD (*P. chrysogenum*; 52kDa) production using the plasmid pET28/a-sorD in *E. coli* BL21 (DE3). M: protein ladder; p: insoluble fraction; sn: soluble fraction; temperature denotes expression temperature after induction with the respective concentration of IPTG.

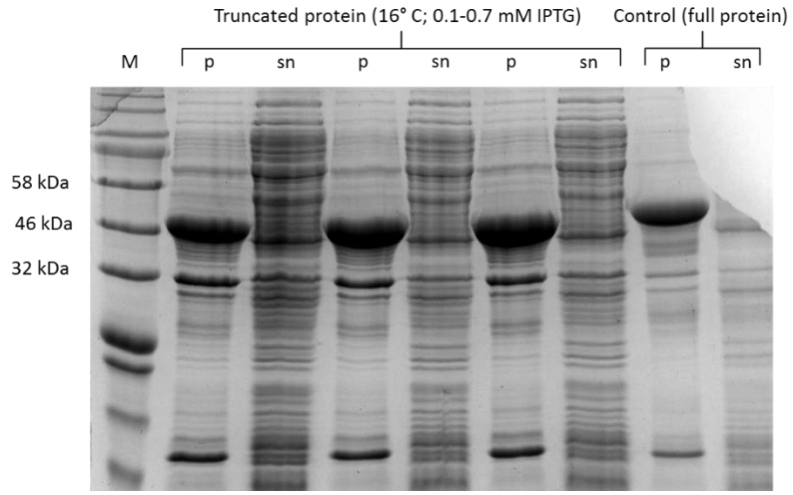

Figure S4: SDS-PAGE of SorD (*P. chrysogenum*; 50kDa) production lacking the first 23 N-terminal amino acid residues production using the plasmid pET28/a-sorD in *E. coli* BL21 (DE3). M: protein ladder; p: insoluble fraction; sn: soluble fraction; temperature denotes expression temperature after induction with the respective concentration of IPTG.

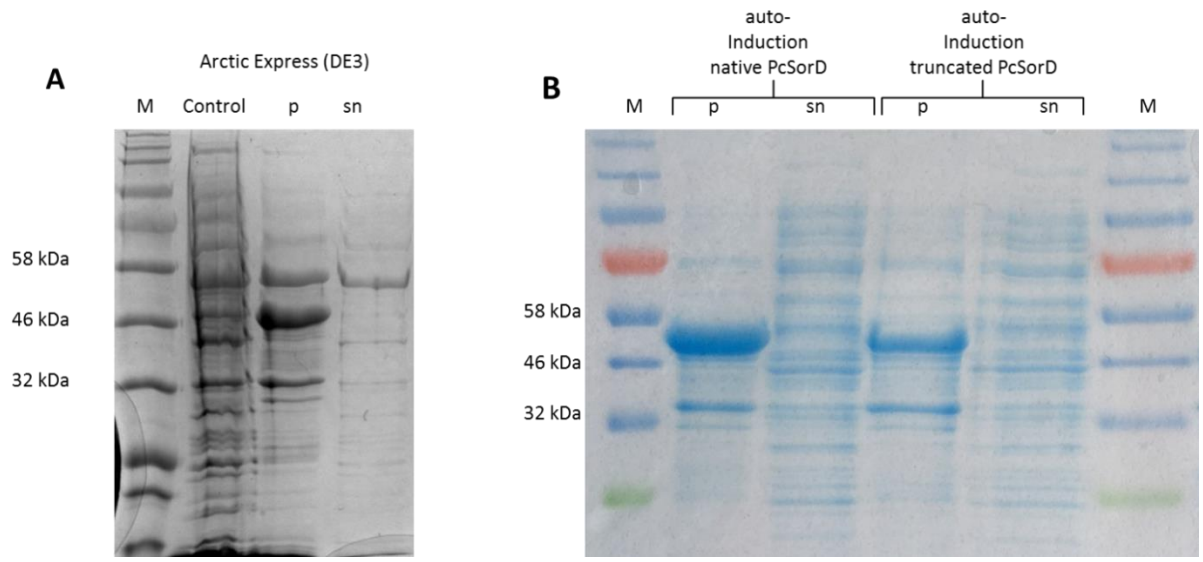

Figure S5: **A** SDS-PAGE of SorD (*P. chrysogenum*; 50kDa) production lacking the first 23 N-terminal amino acid residues production using the plasmid pET28/a-sorD in *E. coli* Arctic express (DE3). Control was taken prior to induction with 0.1 mM IPTG.**B** SDS-PAGE of SorD (*P. chrysogenum*; native 52kDa and truncated 50kDa) using the plasmid pET28/a-sorD in *E. coli* BL21 (DE3) cultivated under autoinduction conditions. Samples were taken after 24h and 48h. Samples shown here represent 48h. M: protein ladder; p: insoluble fraction; sn: soluble fraction.

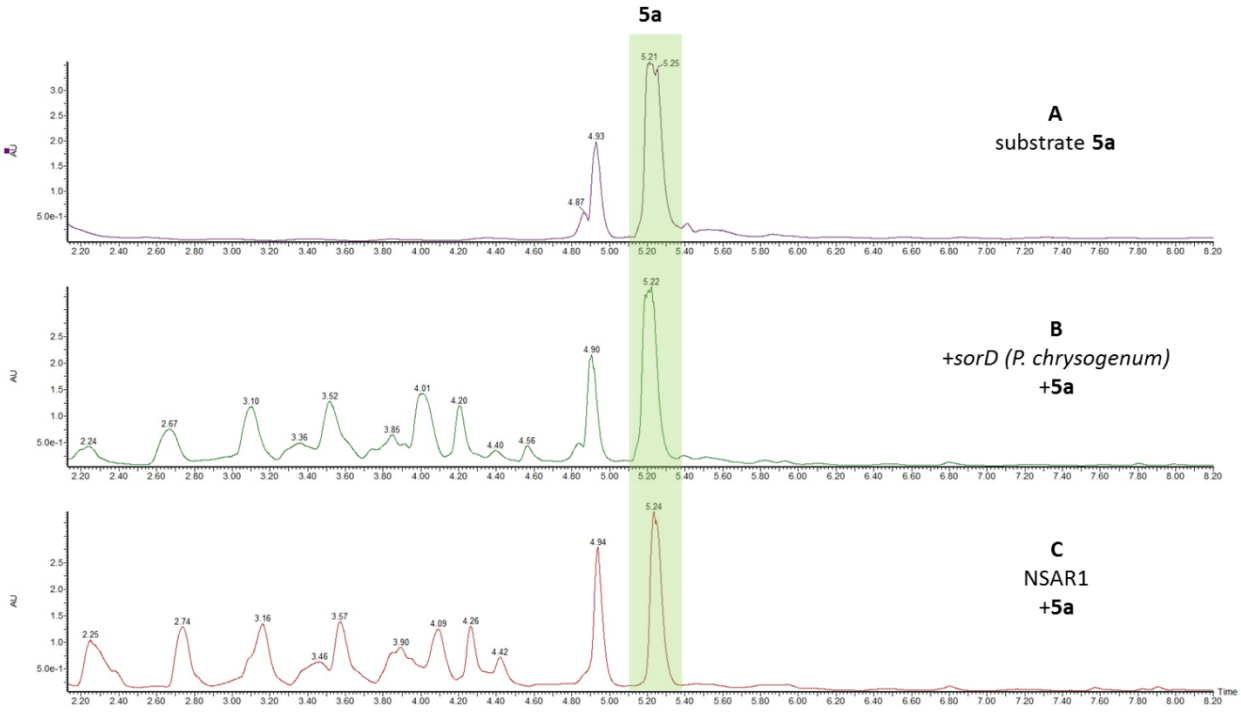

Figure S6: LCMS chromatogram (DAD 210-600 nm) of the epoxysorbicillinol **5a** substrate (**A**), *A. oryzae* expressing *sorD* (*P. chrysogenum*, **B**) and *A. oryzae* NSAR1 (**C**, control) fed with **5a**. No conversion to oxosorbicillinol **6** was observed.

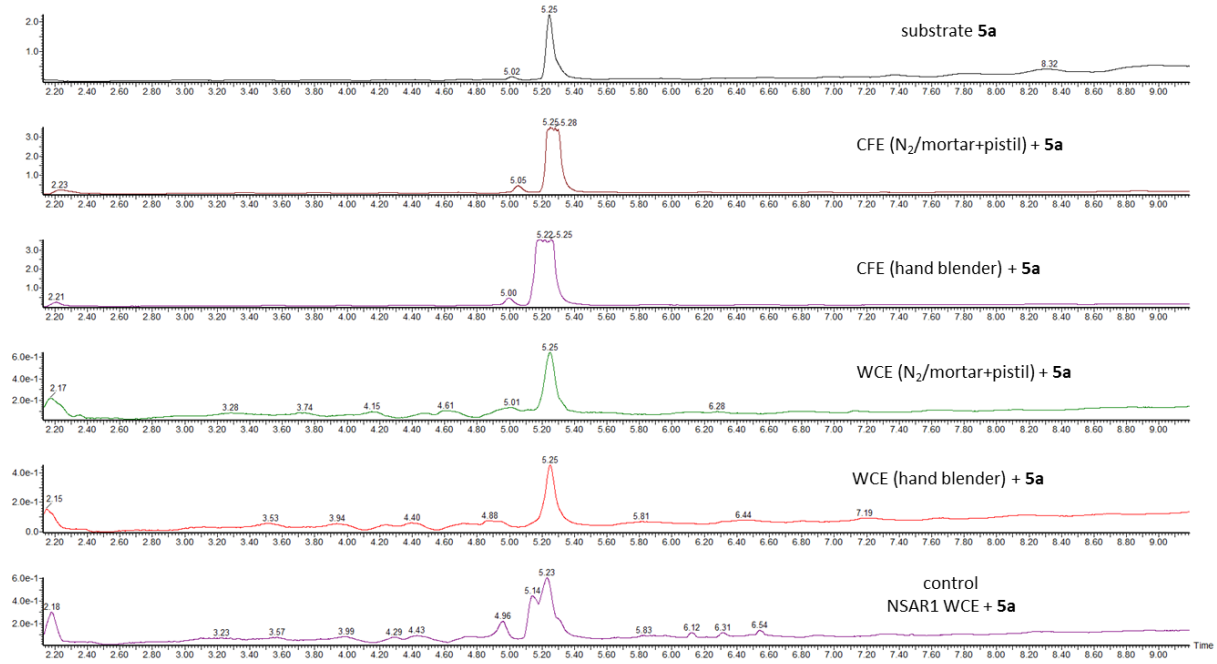

Figure S7: LCMS chromatogram (DAD 210-600 nm) of assays with WCE or CFE of *A. oryzae* expressing *sorD* (*P. chrysogenum*) supplemented with NAD(P)H and epoxysorbicillinol **5a**. No conversion to oxosorbicillinol **6** was observed regardless the method used for sample preparation.

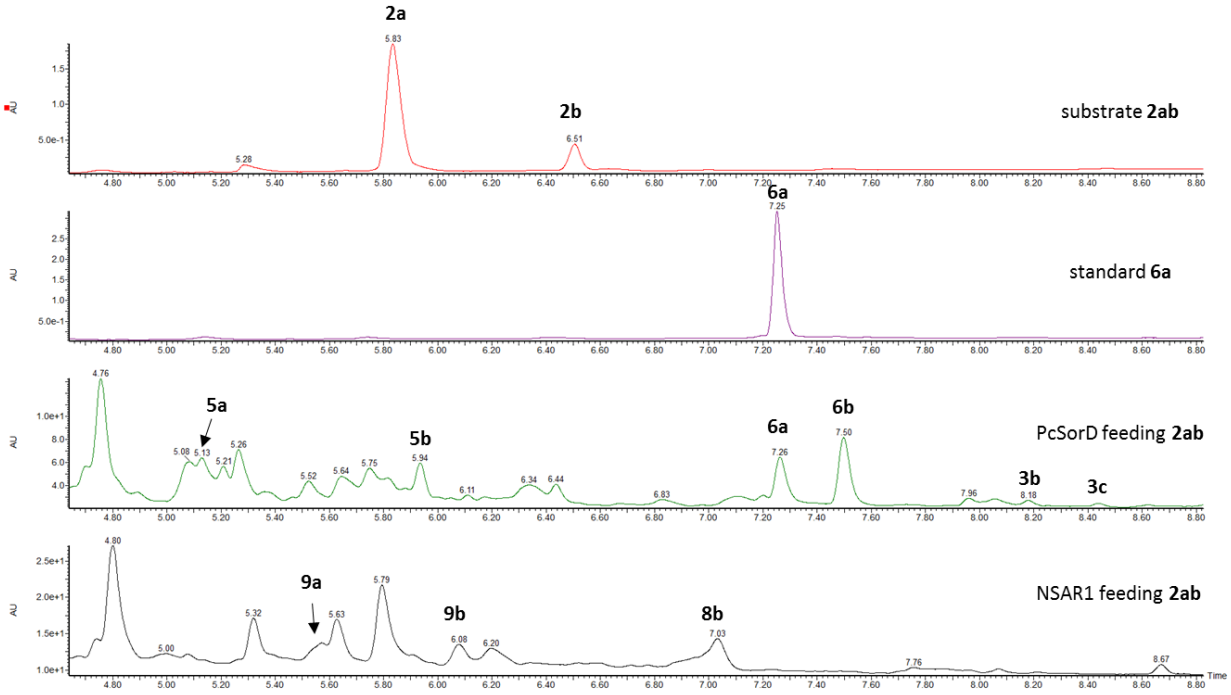

Figure S8: LCMS chromatogram (DAD 210-600 nm) of feeding experiments with **2ab**. In presence of PcSorD **2ab** is converted to epoxides **5ab**, oxosorbicillinols **6ab** and dimeric sorbicillinols **3**. In the NSAR1 control **2** is converted to vertinolides **9** *via* the intermediate **8**.[1]

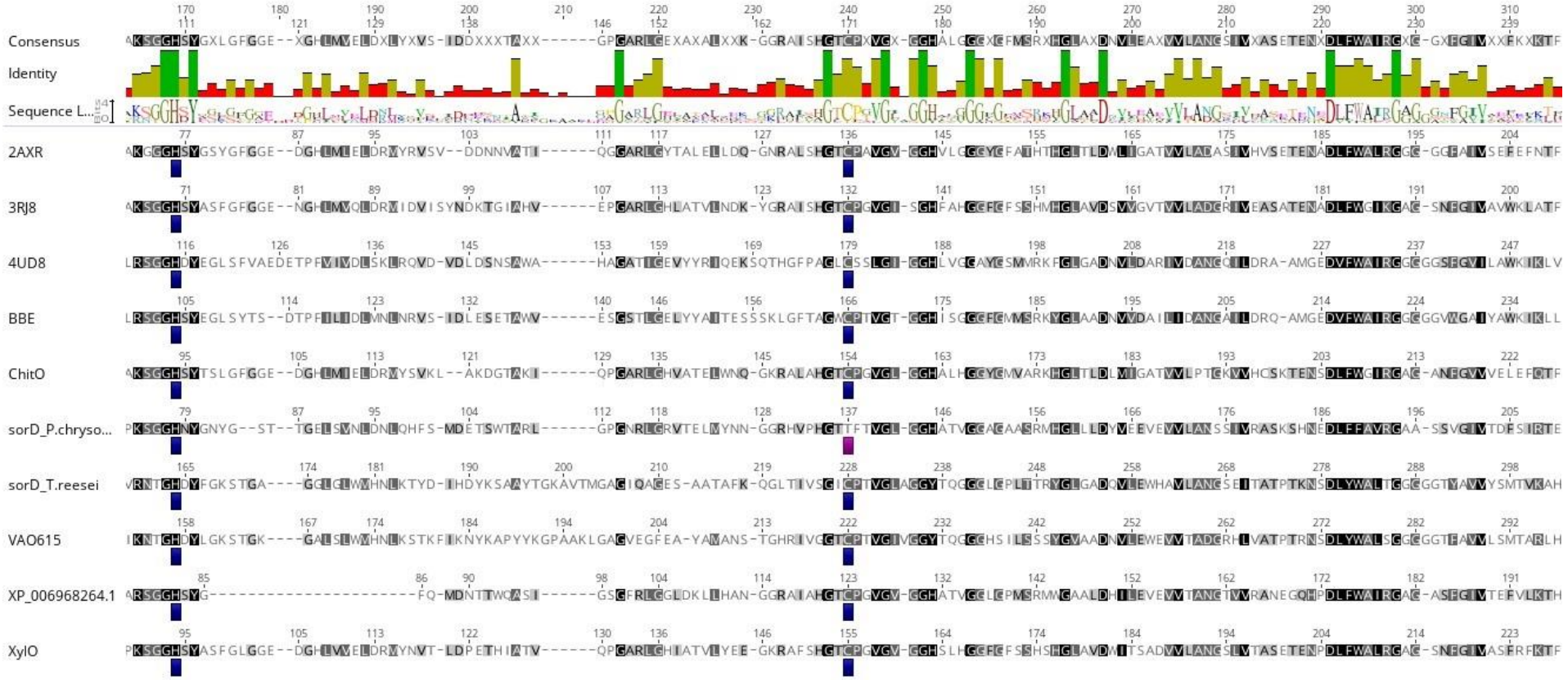

Figure S9: Protein alignment between SorD from *P. chrysogenum,* SorD from *T. reesei* QM6a and FMOs that have been shown to bi-covalently link the flavin cofactor by a conserved histine and cysteine residue (both are highlighted in blue). XP_006968264.1 is an uncharacterized protein, but also displays both conserved residues. SorD from *P. chrysogenum* is lacking the conserved cysteine residue, but displays a threonine residue (purple) instead. Protein alignment was performed using Clustal Omega 1.2.2 in geneious with default parameters. For references and more information about the proteins included in this alignment refer to Figure S11.

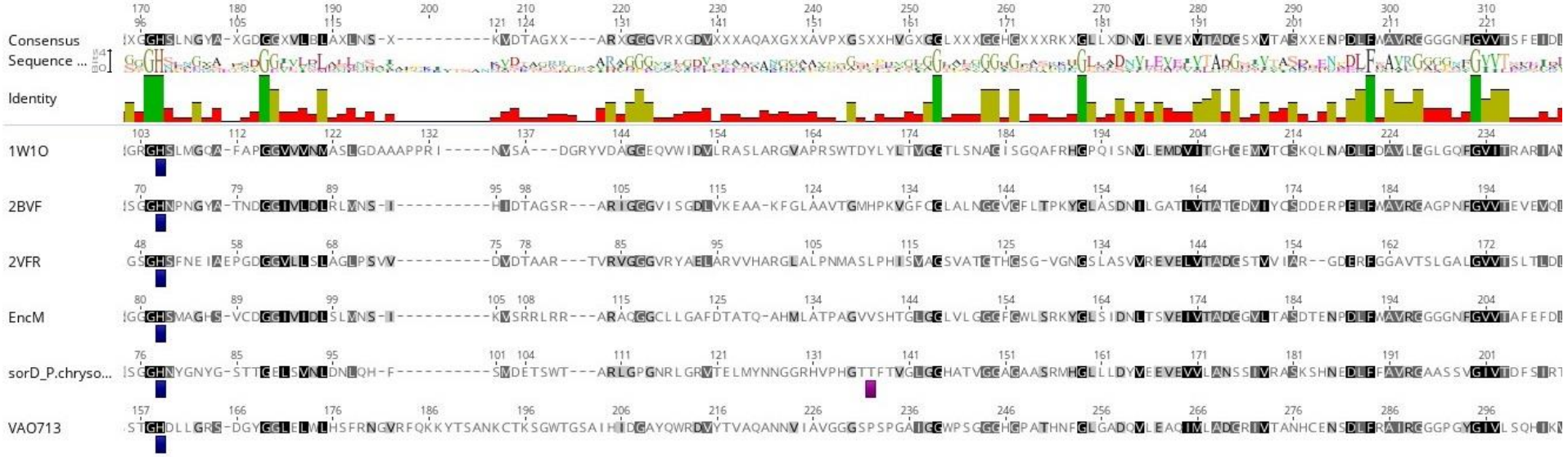

Figure S10: Protein alignment between SorD from *P .chrysogenum* and FMOs that have been shown to mono-covalently link to the flavin cofactor by a conserved histidine residue highlighted in blue and that are the closest relatives to SorD based on the phylogenetic tree in Figure S5.The threonine residue in PcSorD that replaces the conserved cysteine residue found in bi-covalently linked FMOs is highlighted in purple. This residue and its adjacent neighbours are variable throughout the proteins shown. Protein alignment was performed using Clustal Omega 1.2.2 in geneious with default parameters. For references and more information about the proteins included in this alignment refer to Figure S11.

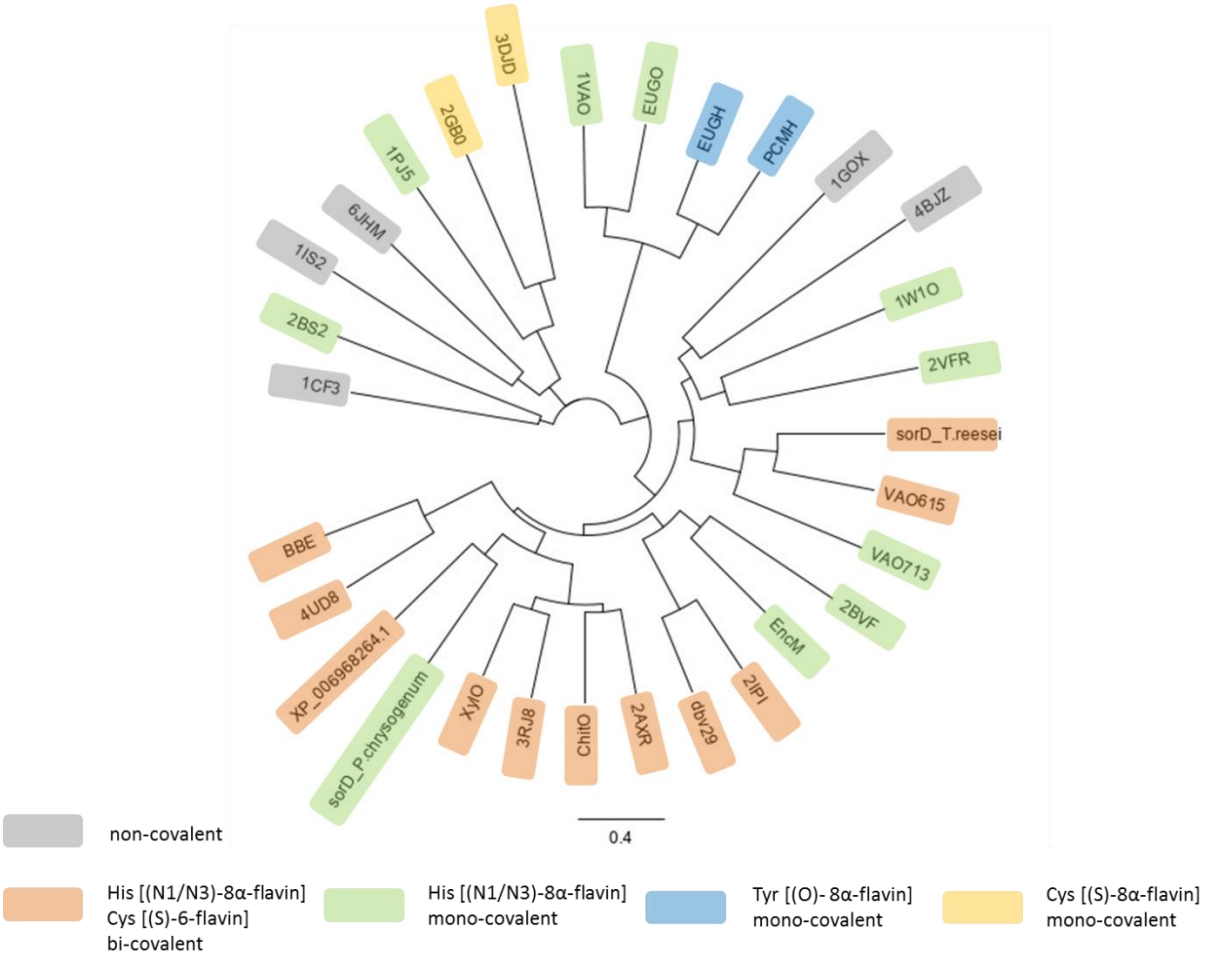

Figure S11: Phylogenetic tree of FMOs that bind the flavin cofactor in either a covalent or non-covalent fashion. Both SorD and XP_006968264.1 are graded based on multiple sequence alignments. The phylogenetic tree was generated in Geneious, based on multiple sequence alignment using Clustal Omega 1.2.2. 1CF3[26]: Glucose oxidase from *Aspergillus niger*, 2BS2[27]: Quinol-fumarate reductase from *Wolinella succinogenes*, 1IS2[28]: Acyl-CoA oxidase from *rattus norvegicus*, 6JHM[29]: Chlorophenol monooxygenase from *Ralstonia pickettii* DTP0602, 1PJ5[30]: N,N-dimethyl oxidase from *Arthrobactor globiformis*, 2GB0[31]: Sarcosine oxidase from *Bacillus* sp. B-0618, 3DJD (Collar *et al*. to be published): Fructosamine oxidase from *A. fumigatus*, 1VAO[32]: Vanillyl-alcohol oxidase from *Pencillium simplicissimum*, EUGO (5FXD)[33]: Eugenol oxidase from *Rhodococcus* sp., EUGH[34]: Eugenol hydroxylase from *Pseudomonas* sp., PCMH (1WVE)[35]: Para-cresol methylhydroxylase from *Pseudomonas putida*, 1GOX[36]: Glycolate oxidase from *Spinacia oleracea*, 4BJZ[37]: 3-Hydroxybenzoate 6-hydroxylase from *Rhodococcus jostii* RHA1, 1W1O[38]: Cytokinin dehydrogenase from *Zae mays*, 2VFR[39]: Alditole oxidase from *Streptomyces coelicolor* A3(2), SorD_T. reesei: FMO from *Trichoderma reesei* QM6a, VAO615(6F72)[6]: VAO-type flavoprotein from *Myceliophthora thermophila* C1, VAO713(6F74)[6]: VAO-type flavoprotein from *Myceliophthora thermophila* C1, 2BVF[40]: 6-Hydroxy-D-nicotine oxidase from *Paenarthrobacter nicotinovorans*, EncM (3W8W)[41]: VAO-type flavoprotein from *Streptomyces maritimus*, 2IPI[42]: Aclacinomycin oxidoreductase from *Streptomyces galilaeus*, dbv29 (2WDW)[43]: Hexose oxidase from *Nonomuraea gerenzanensis*, 2AXR[44]: Glucooligosaccharide oxidase from *Acremonium strictum*, ChitO[45]: Chitooligosaccharide oxidase from *Fusarium graminearum*, 3RJ8 (Duskova *et al*. to be published): Carbohydrate oxidase from *Microdochium nivale*, XylO (5K8E)[7]: Xylooligosaccharide oxidase from *myceliophthora thermo*phila C1, SorD_P.chrysogenum: FMO from *Penicillium chrysogenum*, XP_006968264.1: uncharacterized FMO from *T. reesei* QM6a, 4UD8[46]: Oxidoreductase from *Arabidopsis thaliana*, BBE (4EC3)[47]: Berberine bridge enzyme from *Eschscholzia californica.*

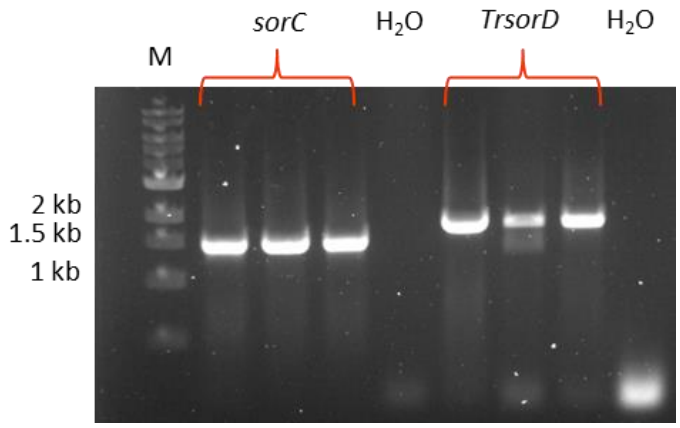

Figure S12: Confirmation of integration of *sorC* and *sorD* (*T.*reesei) into fungal transformants additionally expressing *sorAB* by PCR. The three transformants screened successfully integrated the genes. 1 % agarose gel run at 110V for 25 min. M: DNA marker, H_2O: negative control without template.

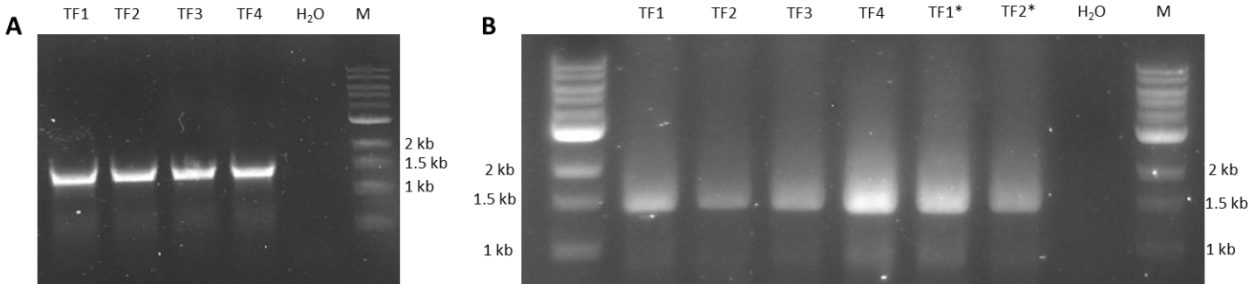

Figure S13: Confirmation of integration of *sorC* (**A**) and *sorD* (*P. chrysogenum*; **B**) into fungal transformants by PCR. The four transformants shown(TF1-TF4; also co-expressing both PKS genes *sorA* and *sorB*) successfully integrated the genes. The two transformants TF1* and TF2* solely expressing *PcsorD* were used for feeding studies and cell free extract assays using epoxysorbicillinol **5a** as substrate. 1 % agarose gels run at 110V for 20 min. M: DNA marker, H_2O: negative control without template.

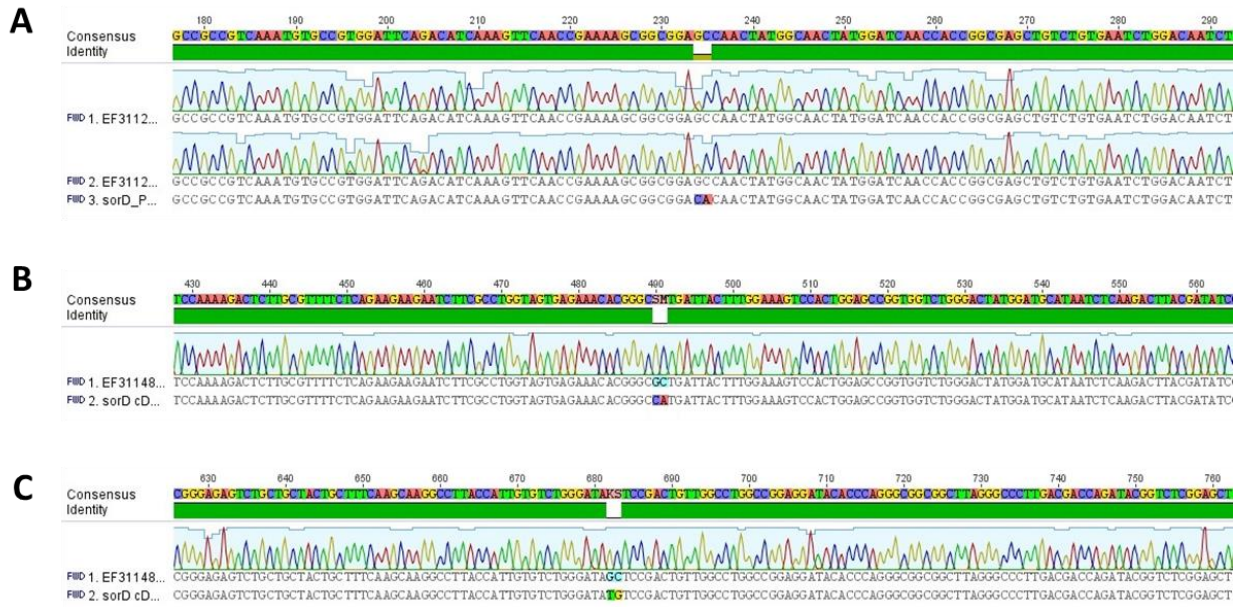

Figure S14: Mutation of His78→Ala78 in *P. chrysogenum* (**A**) , His164→Ala164 in *T. reesei* (**B**) and Cys228→Ala228 in *T. reesei* (**C**) confirmed by sequencing.

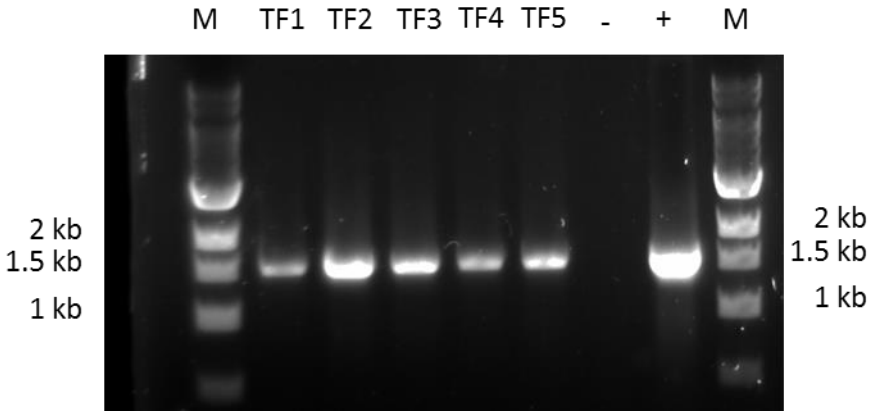

Figure S15: Confirmation of integration of *sorD* (*P. chrysogenum*; His78→Ala78) into fungal transformants additionally expressing *sorABC* by PCR. The five transformants screened successfully integrated the gene. 1 % agarose gel run at 110V for 25 min. M: DNA marker, TF: transformant, -: negative control without template, +: positive control using pTYGSmet-*sorD* (*P. chrysogenum*; His78→Ala78) as template.

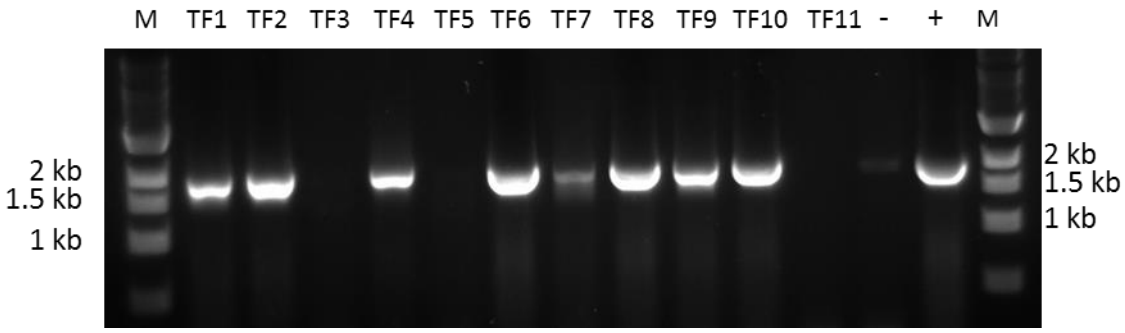

Figure S16: Confirmation of integration of *sorD* (*T. reesei*; His164→Ala164 and Cys228→Ala228) into fungal transformants additionally expressing *sorABC* by PCR. Eight transformants successfully integrated the gene. 1 % agarose gel run at 110V for 25 min. M: DNA marker, TF: transformant, -: negative control without template, +: positive control using pTYGSmet-*sorD* (*T. reesei*; His164→Ala164 and Cys228→Ala228) as template.

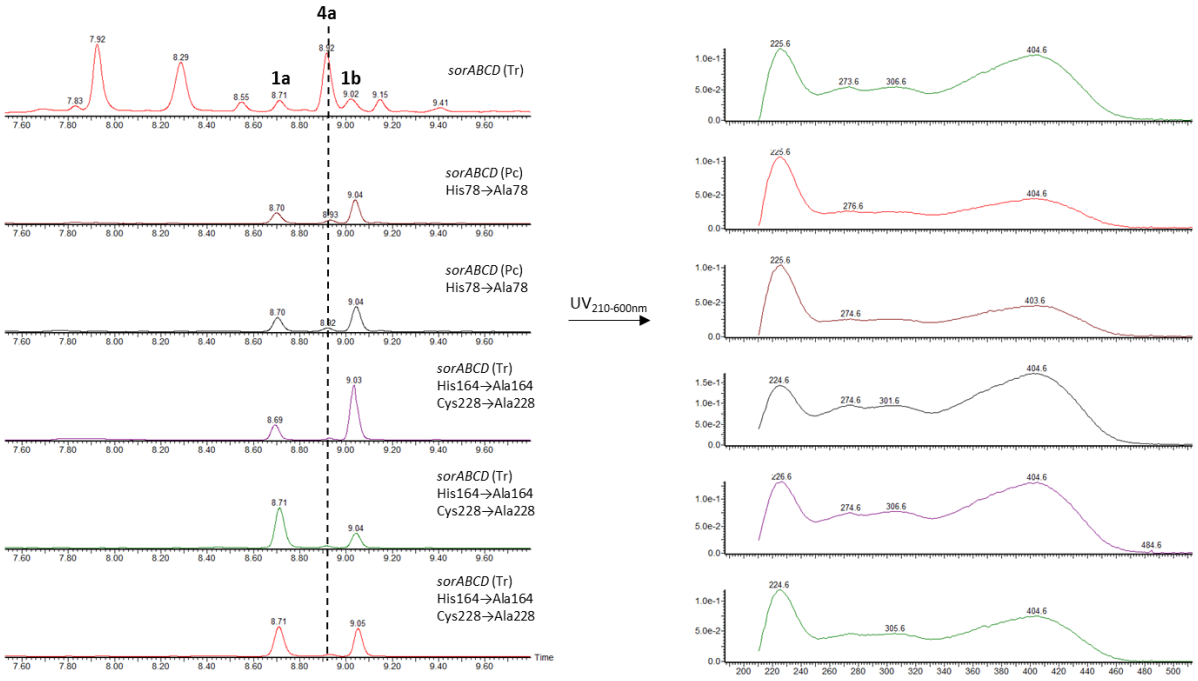

Figure S17: Comparison of LCMS data ($UV_{210-600nm}$) showing the reproducible production of Michael-dimer **4a** by individual transformants expressing *sorABCD* (Tr; His164→Ala164 and Cys228→Ala228) or *sorABCD* (Pc; His78→Ala78). A transformants expressing the native *sorABCD* (Tr) is shown as a control. All peaks highlighted as **4a** share the same UV-absorption.

Table S1: Media used during this study.

Media	**Components**
2TY medium	16 g/L tryptone, 10 g/L yeast extract, 5 g/L NaCl
CZD/S1 agar	35 g/L Czapek Dox broth, 182.2 g/L D-sorbitol, 1 g/L ammonium sulphate, 1.5 g/L-methionine, 15 g/L agar
CZD/S1 soft agar	35 g/L Czapek Dox broth, 182.2 g/L D-sorbitol, 1 g/L ammonium sulphate, 1.5 g/L-methionine, 8 g/L agar
CZD/S1 agar w/o methionine	35 g/L Czapek Dox broth, 182.2 g/L D-sorbitol, 1 g/L ammonium sulphate, 15 g/L agar
CZD/S1 soft agar w/o methionine	35 g/L Czapek Dox broth, 182.2 g/L D-sorbitol, 1 g/L ammonium sulphate, 8 g/L agar
DPY medium	20 g/L dextrine from potato starch, 10 g/L polypeptone, 5 g/L KH_2PO_4, 0.5 g/L $MgSO_4 \cdot H_2O$
GN medium	20 g/L D (+)-glucose monohydrate, 10 g/L nutrient broth No. 2 from oxoid (Thermo Scientific)
LB agar	5 g/L yeast extract, 10 g/L tryptone, 5 g/L NaCl, 15 g/L agar
LB medium	5 g/L yeast extract, 10 g/L tryptone, 5 g/L NaCl
LBE-5052 medium	5 g/L yeast extract, 10 g/L tryptone, 5 g/L glycerol, 0.5 g/L D(+)-Glucose monohydrate, 2 g/L lactose monohydrate, 0.7 g/L sodium sulfate, 2.5 g/L ammonium chloride, 1mL magnesium sulfate hexahydrate (2M), 100 mL phosphate buffer (50mM), 1 mL metal mix
Metal mix	198 mg Manganese-(II)-chloride tetrahydrate 288 mgZinc sulfate heptahydrate 48 mg Cobalt-(II)-chloride hexahydrate 48 mg Nickel-(II)-chloride hexahydrate 811 mg Iron-(III)-chloride 0.5 mL HCl (Conc.)

	Fill up to 100 mL with pure water
Phosphate buffer (50mM)	13.6 g/L monopotassium phosphate, 69.6 g/L dipotassium phosphate
SM-ura agar	1,7 g/L yeast nitrogen base, 20 g/L D (+)-glucose monohydrate, 5 g/L ammonium sulphate, 0.77 g/L complete supplement mixture minus uracil (Q biogene), 25 g/L agar
SOB medium	20 g/L tryptone, 5 g/L yeast extract, 584 mg/L NaCl, 186 mg/L KCl
SOC medium	937.5 mL/L SOB medium, 12.5 mL/L $MgCl_2$, 50 mL/L glucose (20 %) components were autoclaved separately and sterile filtrated after mixing
TB medium	24 g/L yeast extract, 12 g/L tryptone, 4 g/L glycerol, 100 mL KPI buffer (10x)
KPI buffer (10x)	23.12 g/L monopotassium phosphate, 125.41 g/L dipotassium phosphate
YPAD agar	10 g/L yeast extract, 20 g/L tryptone, 0.3 g/L adenine, 20 g/L D (+)-glucose monohydrate, 15 g/L agar
YPAD medium	10 g/L yeast extract, 20 g/L tryptone, 0.3 g/L adenine, 20 g/L D (+)-glucose monohydrate

Table S2: Primers used during this study.

Primer name	Sequence (5' to 3')
SorA P1	GCCAACTTTGTACAAAAAAGCAGGCTCCGCATGAAGCTGACGGCCCTCAA
SorA P3	TTGCAAATGTCTACGTCGAGG
SorA P6	CGAGATTATACAGGATAGGCTC
SorA P7	TCGAAGACTCATTGCGGCTGTT
SorA P9	CCTGTACTCATGGCCTTAATGC
SorA P10	ATCTGCATCTTTATCGGGGAAAT
SorB P1	GCCAACTTTGTACAAAAAAGCAGGCTCCGCATGGCGGCCTCAAGTACACG
SorB P2	ATTAACACTAAACGCCAGGTCTTGGATATCGAGATTGCTGTGAGAGTAAA
SorB P3	GCAATCTCGATATCCAAGACC
SorB P4	GTCACCAAGCGTAGACTGTAG
SorB P5	CCTTAAGTTCCTACAGTCTACGCTTGGTGACGAGGACGTTCACGACTCTT
SorB P6	TGCCAACTTTGTACAAGAAAGCTGGGTCGGTCATCGCAAAAAGCCGCTAT
SorC F	TTCTTTCAACACAAGATCCCAAAGTCAAAGATGGAGCCGAACAATCATCAC
SorC R	TTTCATTCTATGCGTTATGAACATGTTCCCTCTAATGCTTCTCTAACACCT
SorD F (*T. reesei*)	CGACTGACCAATTCCGCAGCTCGTCAAAGGATGTACGCCCCCCCTTTTGT
SorD R (*T. reesei*)	AGGTTGGCTGGTAGACGTCATATAATCATATTACGAGACTCGGCAAAGGC
SorD F (*P. chrysogenum*)	TTCTTTCAACACAAGATCCCAAAGTCAAAGATGCAGGCCGCCAGTGCATT
SorD R (*P. chrysogenum*)	TTCATTCTATGCGTTATGAACATGTTCCCTCTAGGACAGAGGTGGGATAC
SorD NdeI (*P. chrysogenum*)	GGGAATTCCATATGCAGGCCGCCAGTGCATTTGC
SorD NotI (*P. chrysogenum*)	TTCCTTTTTTGCGGCCGCCTAGGACAGAGGTGGGATAC
SorD NdeI short (*P. chrysogenum*)	GGGAATTCCATATGTTTCCAAACCAAGCCAACTATT
SorD FAD F (*P. chrysogenum*)	GAAAAGCGGCGGACACAACTATGG
SorD FAD R (*P. chrysogenum*)	CATAGTTGCCATAGTTGTGTCCGCCG
SorD FAD F1 (*T. reesei*)	TGAGAAACACGGGCCATGATTACT
SorD FAD R1 (*T. reesei*)	CTTTCCAAAGTAATCATGGCCCGT
SorD FAD F2 (*T. reesei*)	CATTGTGTCTGGGATATGTCCGA
SorD FAD R2 (*T. reesei*)	GGCCAACAGTCGGACATATCCCA
(XP_006968264.1) F	ACAGCTACCCCGCTTGAGCAGACATCACCGATGGGCAACTCGAATTCCAC
(XP_006968264.1) R	TACGACAATGTCCATATCATCAATCATGATTCATGGCAAATCGACGCTCT

Table S3: Plasmids used during this study.

Plasmid	**Features**
pET28/a (Novagen)	*kan^{R}pBR322 ori LacI f1 ori pT7 His-Tag*
pET28/a-*sorD*(*P. chrysogenum*)	encodes for *sorD*(*P. chrysogenum*) with N-terminal his$_6$-tag; cloned from pMA-T-*sorD*(*P. chrysogenum*); also with first 23 amino acid residues removed
pE-YA[48]	*kan^R pUC ori 2µ ori URA3 ccdB*
pE-YA-*sorA*	*sorA* inserted by LR-recombination
pE-YA-*sorB*	*sorB* inserted by LR-recombination
pTYGSarg/ade/met[48]	*PamyB Padh Peno PgdpA amp^R ColE1 2µ ori URA3 ccdB argB/adeA/sC*
pTYGSade-*sorA*	*sorA* under control of *PamyB*
pTYGSade-*sorD*(*T. reesei*)	*sorD*(*T. reesei*)under control of *Padh*
pTYGSade-*sorAD*(*T. reesei*)	*sorA* under control of *PamyB, sorD* (*T. reesei*) under control of *Padh*
*a version of this vector with His164→Ala164 and Cys228→Ala228 was also created	
pTYGSarg-*sorB*	*sorB* under control of *PamyB*
pTYGSarg-*sorC*	*sorC* under control of *Padh*
pTYGSarg-*sorBC*	*sorB* under control of *PamyB, sorC* under control of *Padh*
pTYGSmet-*sorD*(*P. chrysogenum*)	*sorD* (*P. chrysogenum*) under control of *Padh*
*a version of this vector with His78→Ala78 was also created	
pTYGSmet-(XP_006968264.1)	(XP_006968264.1) under control of *PgdpA*

Table S4: Fungal strains used during this study.

Fungal strain	**genotype**
A. oryzae NSAR1	*argB$^-$, adeA$^-$, sC$^-$, niaD$^-$*
A. oryzae-sorABC	*+sorA, +sorB, +sorC, sC$^-$, niaD$^-$*
A. oryzae-sorABCD(*T. reesei*)	*+sorA, +sorB, +sorC, +sorD, sC$^-$, niaD$^-$*
*a version of this strain with His164→Ala164 and Cys228→Ala228 was also created	
A. oryzae-sorABCD(*P. chrysogenum*)	*+sorA, +sorB, +sorC, +sorD*(*P. chrysogenum*), *niaD$^-$*
*a version of this strain with His78→Ala78 was also created	
A. oryzae-sorD(*P. chrysogenum*)	*+sorD*(*P. chrysogenum), niaD$^-$*
A. oryzae-sorABCD(*T. reesei*) - (XP_006968264.1)	*+sorA, +sorB, +sorC, +sorD,* (XP_006968264.1), *niaD$^-$*

Compound Physical data

Compounds identified by NMR-analysis

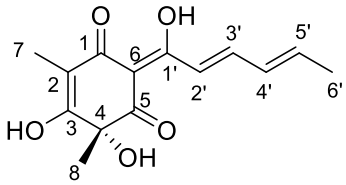

Oxosorbicillinol **6a**

Chemical Formula: $C_{14}H_{16}O_5$
Exact Mass: 264,0998

$UV_{\lambda max}$ (MeOH): 229 nm, 306 nm, 374 nm

HRMS (ESI) *m/z* $(M+H)^+$ calculated for $C_{14}H_{17}O_5$: 265.1076, found: 265.1079

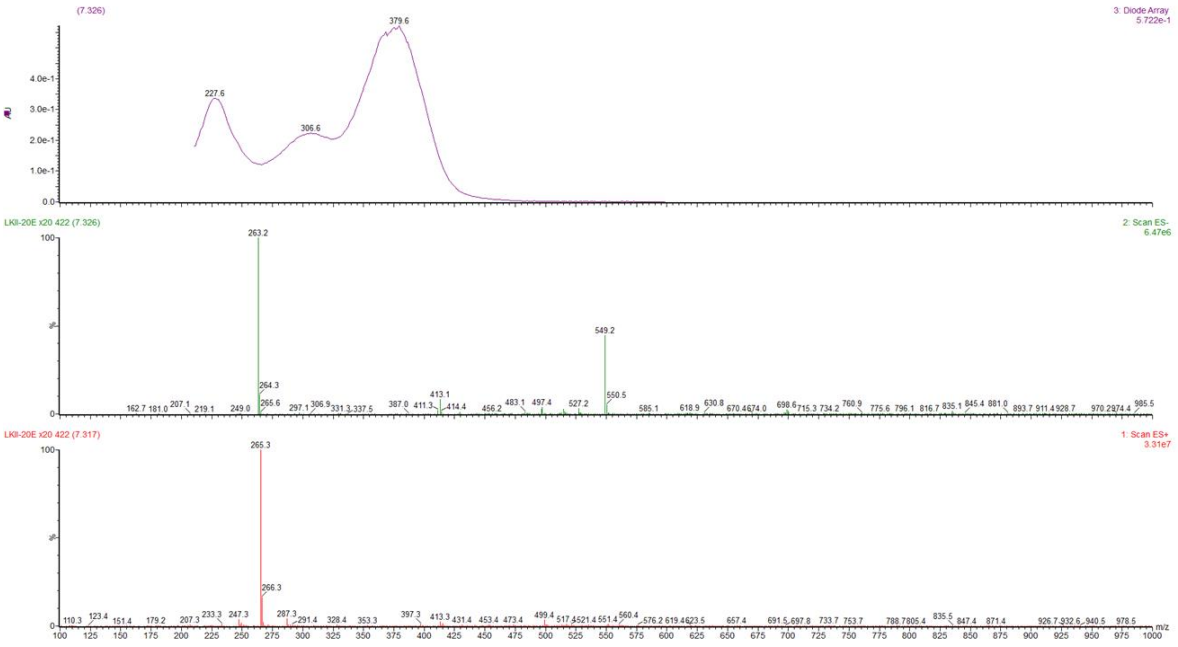

Figure S18: UV-absorption (top) and fragmentation pattern of **6a** in ES^-(middle) and ES^+ (bottom). Retention time is shown in brackets at the top left hand corner.

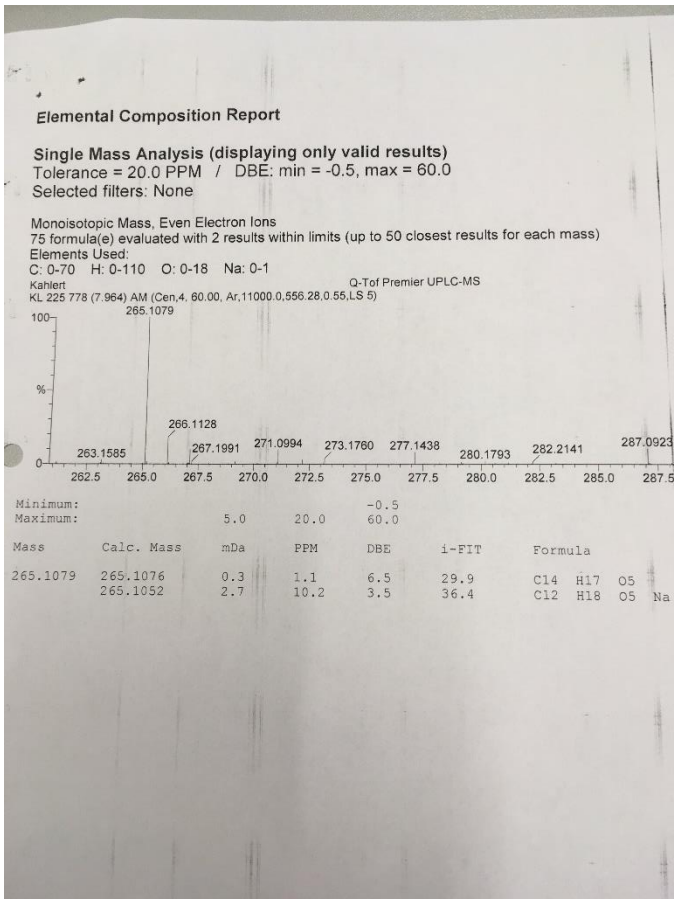

Figure S19: HRMS data of **6a**.

Table S5: Summarized NMR-data for **6a** recorded in acetonitrile-D_3.

Position	δ_H	M	J_{H-H}/Hz	δ_C	HSQC	HMBC H to C	H-H COSY
1		-	-	192.3	-	-	-
2	-	-	-	105.7	-	-	-
3	-	-	-	171.8	-	-	-
4	-	-	-	76.5	-	-	-
5	-	-	-	197.2	-	-	-
6	-	-	-	105.5	-	-	-
7	1.77	s	-	7.4	CH_3	1, 2, 3, 6	-
8	1.48	s	-	29.7	CH_3	3, 4, 5,	-
1‘	-	-	-	185.3	-	-	-
2‘	7.33	d	15.2	124.1	CH	1‘, 3‘, 4‘	3‘
3‘	7.48	m	-	145.4	CH	1‘, 2‘, 4‘, 5‘, 6‘	2‘, 4‘
4‘	6.41	m	-	131.9	CH	6‘, 5‘, 3‘	3‘, 5‘
5‘	6.33	m	-	142.4	CH	6‘, 4‘, 3‘	4‘, 6‘
6‘	1.88	d	5.9	19.0	CH_3	3‘ 4‘, 5‘	5‘

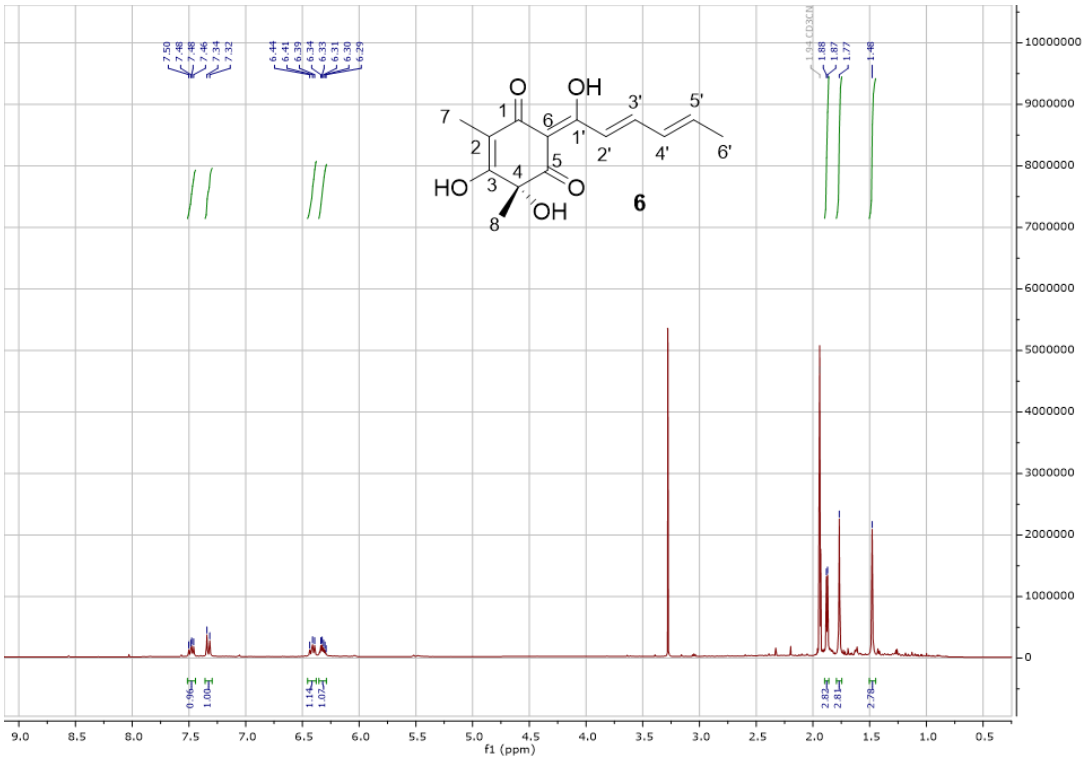

Figure S20: ^{1}H-NMR spectrum for **6a** recorded at 600 MHz in acetonitrile-D_3.

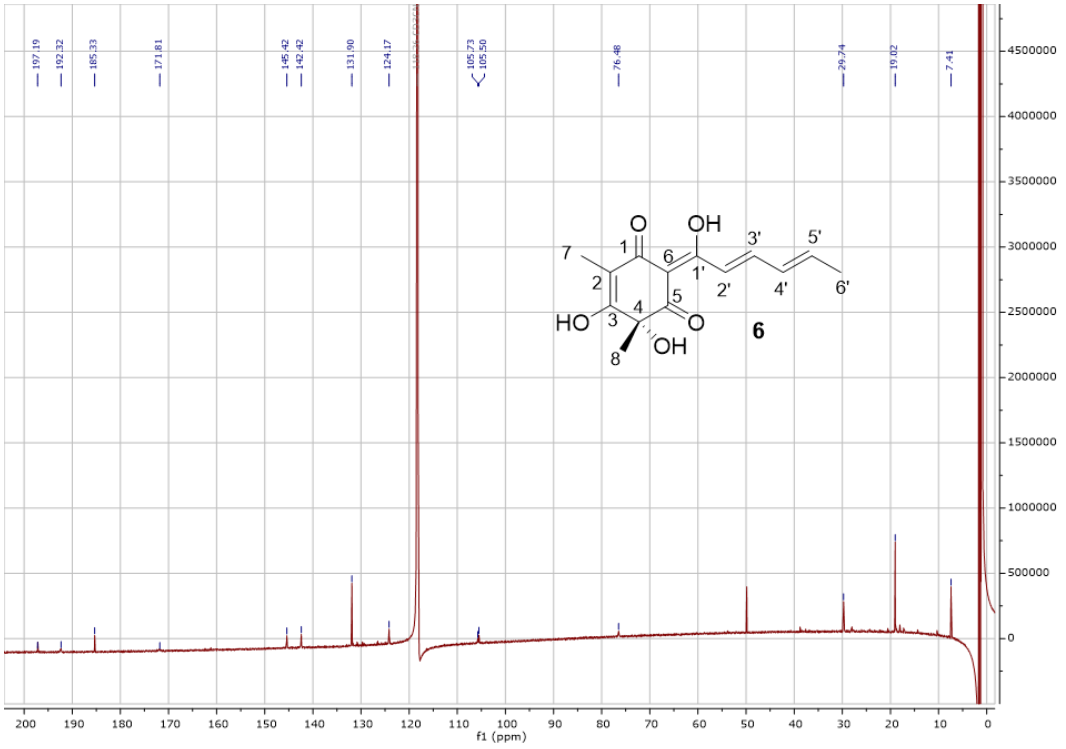

Figure S21: ^{13}C-NMR spectrum for **6a** recorded at 125 MHz in acetonitrile-D_3.

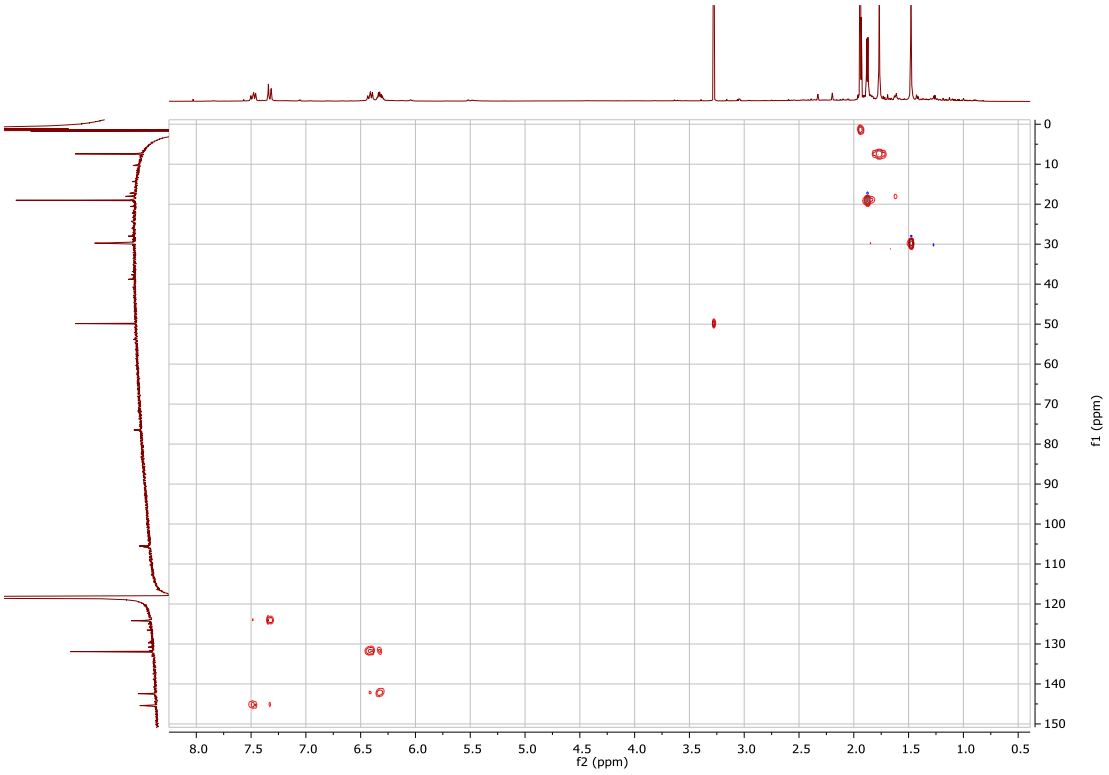

Figure S22: HSQC-spectrum for **6a** recorded in acetonitrile-D_3.

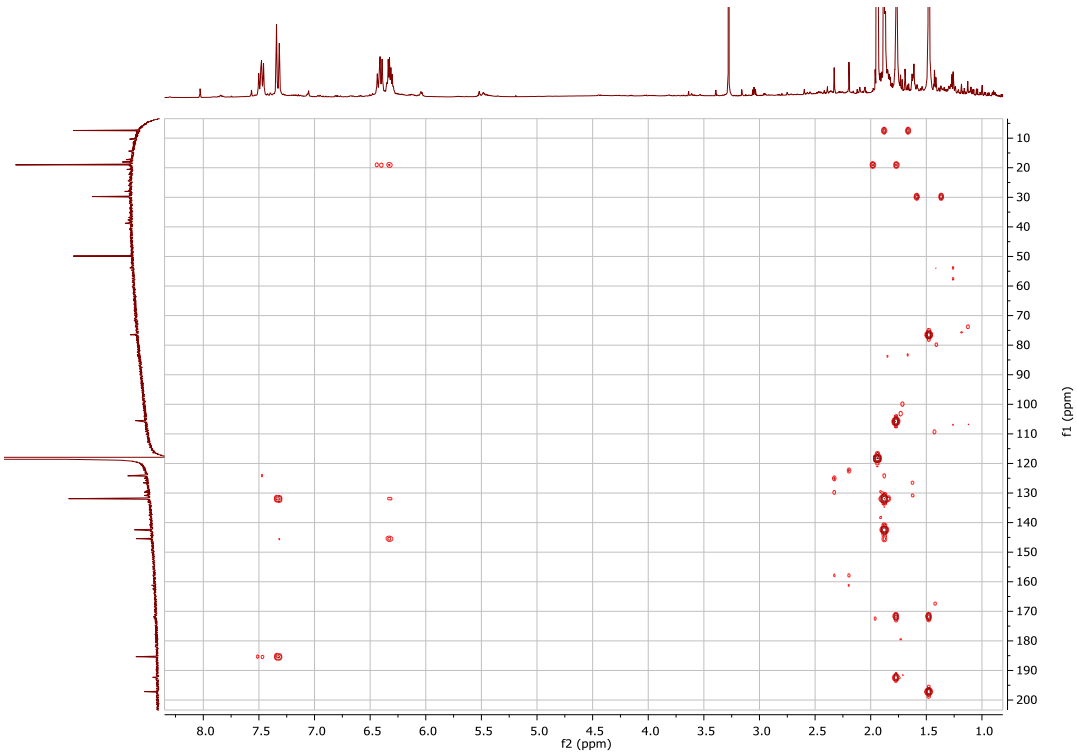

Figure S23: HMBC-spectrum for **6a** recorded in acetonitrile-D_3.

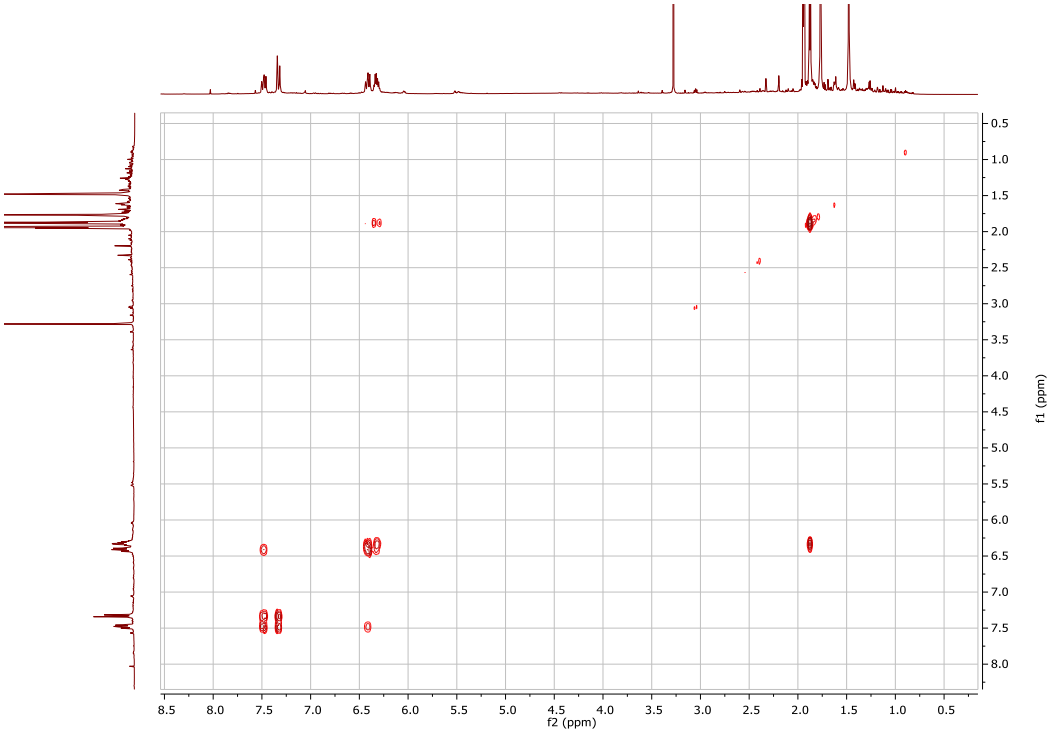

Figure S24: ^{1}H-^{1}H COSY-spectrum for **6a** recorded in acetonitrile-D_3.

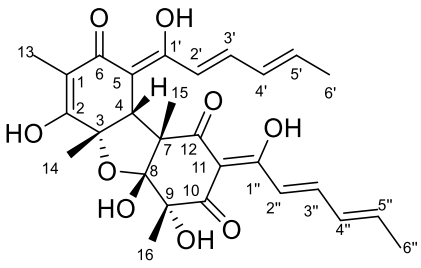

Bisvertinolone **7a**

Chemical Formula: $C_{28}H_{32}O_9$
Exact Mass: 512,2046

$UV\lambda_{max}$ (MeOH): 225 nm, 269 nm, 380 nm

HRMS (ESI) *m/z* (*M*+H)$^+$ calculated for $C_{28}H_{33}O_9$: 513.2125, found: 513.2125

Stereochemistry of **7a** and related Michael-dimers is based on Hirota *et al*[49]. and Gulder *et al.*[50] NMR data shown below are in agreement with these reports.

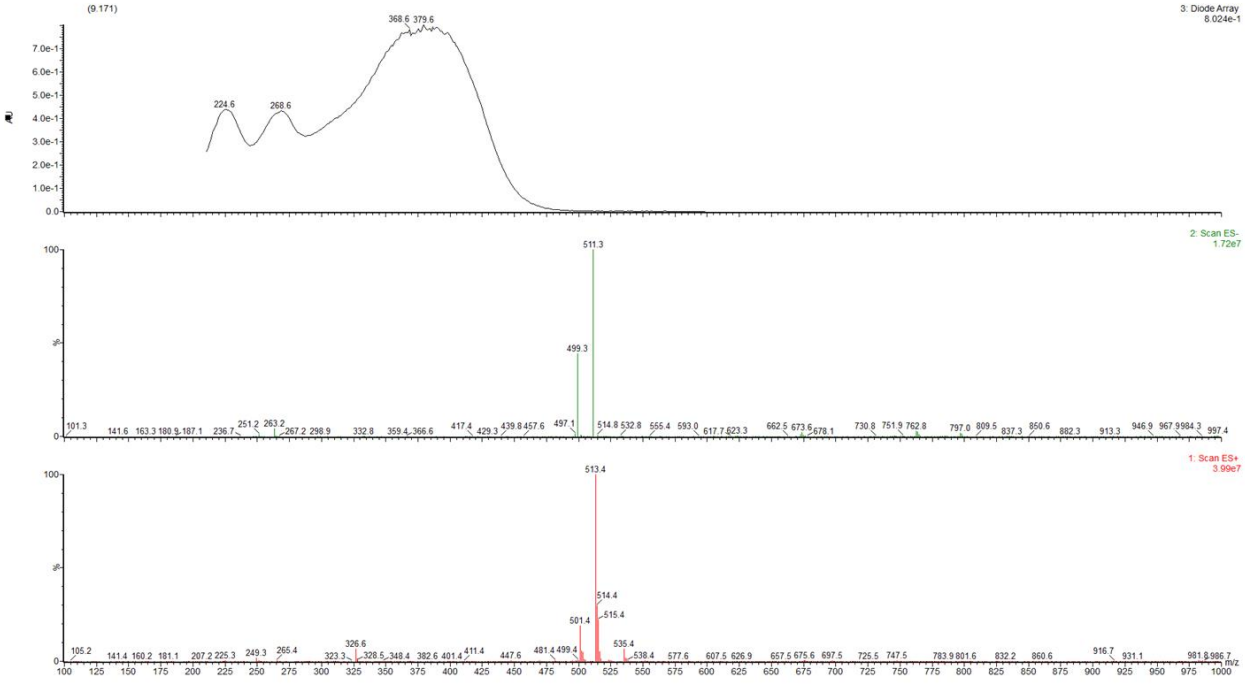

Figure S25: UV-absorption (top) and fragmentation pattern of **7a** in ES^- (middle) and ES^+ (bottom). Retention time is shown in brackets at the top left hand corner. Note: contains impurities of 2', 3'-dihydrobisvertinol **4b** or 2'', 3''-dihydrobisvertinol **4b'**.

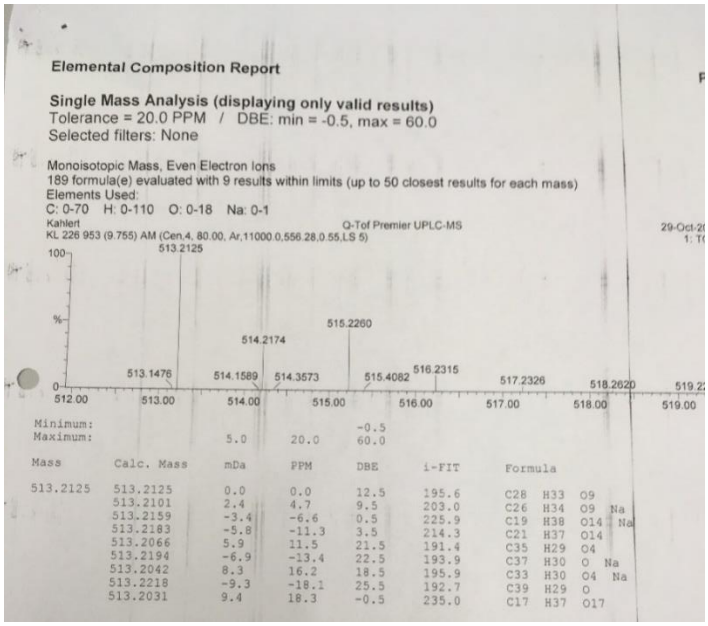

Figure S26: HRMS data of **7a**.

Table S6: Summarized NMR-data for **7a** recorded in $CDCl_3$.

Position	δ_H	M	J_{H-H}/Hz	δ_C	HSQC	HMBC H to C	H-H COSY
1	-	-	-	111.1	-	-	-
2	-	-	-	163.4	-	-	-
3	-	-	-	79.8	-	-	-
4	3.74	s	-	54.5	CH	1‘, 2, 3, 5, 6, 7, 12, 14, 15,	-
5	-	-	-	99.9	-	-	-
6	-	-	-	191.4	-	-	-
7	-	-	-	59.9	-	-	-
8	-	-	-	104.4	-	-	-
9	-	-	-	79.0	-	-	-
10	-	-	-	196.7	-	-	-
11	-	-	-	107.4	-	-	-
12	-	-	-	200.0	-	-	-
13	1.50	s	-	7.1	CH_3	1, 2, 6	-
14	1.44	s	-	25.8	CH_3	2, 3	-
15	1.46	s	-	18.8	CH_3	4, 7, 8, 12	-
16	1.38	s	-	23.2	CH_3	8, 9, 10	-
1‘	-	-	-	170.6	-	-	-
2‘	6.39	m	-	120.1	CH	1‘	3‘
3‘	7.32	dd	14.7, 11.0	139.9	CH	1‘, 5‘	2‘, 4‘
4‘	6.30	m	-	131.2	CH	1‘, 6‘	3‘, 5‘
5‘	6.14	m	-	137.8	CH	6‘, 4‘, 3‘	6‘, 4‘
6‘	1.88	d	6.5	19.0	CH_3	4‘, 5‘	5‘
1‘‘	-	-	-	185.6	-	-	-
2‘‘	7.41	d	11.7	121.9	CH	1‘‘, 4‘‘, 6‘‘	3‘‘
3‘‘	7.58	dd	15.2, 9.7	148.6	CH	1‘‘, 5‘‘	2‘‘, 4‘‘
4‘‘	6.37	m	-	131.4	CH	2‘‘, 3‘‘, 5‘‘, 6‘‘	3‘‘, 5‘‘
5‘‘	6.36	m	-	144.4	CH	3‘‘, 4‘‘, 6‘‘,	4‘‘, 6‘‘
6‘‘	1.93	d	5.1	19.4	CH_3	4‘‘, 5‘‘	5‘‘

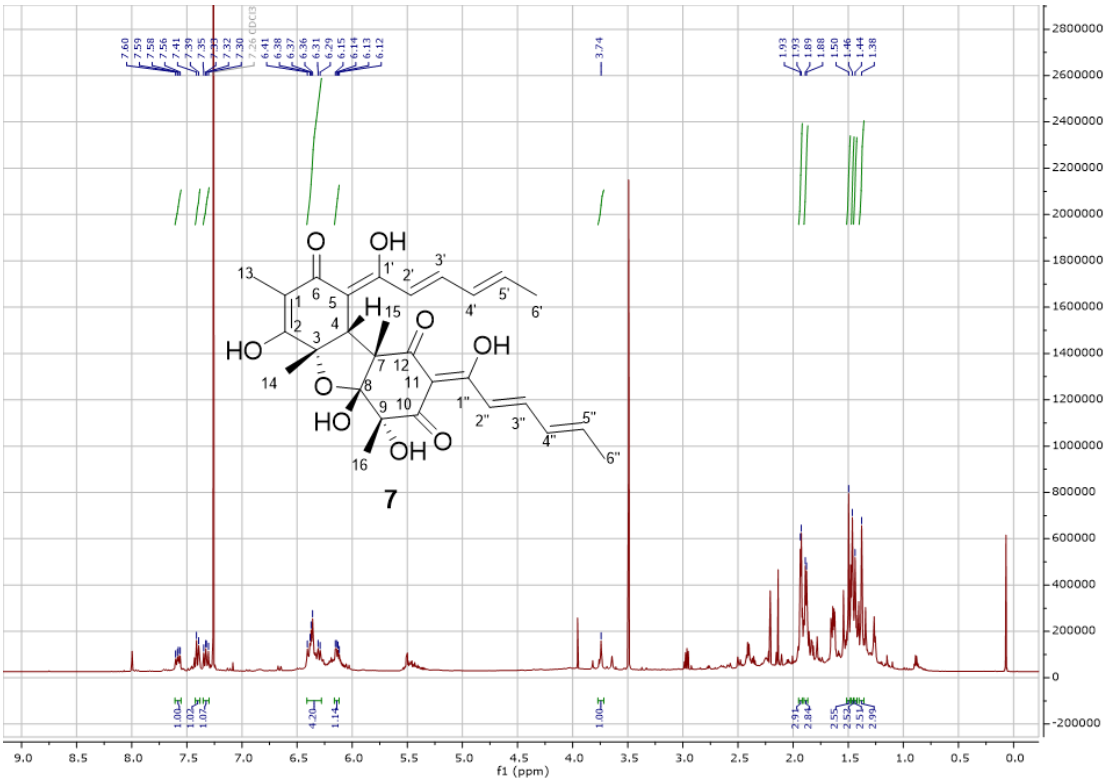

Figure S27: ^{1}H-NMR spectrum for **7a** recorded at 600 MHz in $CDCl_3$. Note: contains impurities of 2', 3'-dihydrobisvertinol **4b** or 2'', 3''-dihydrobisvertinol **4b'**.

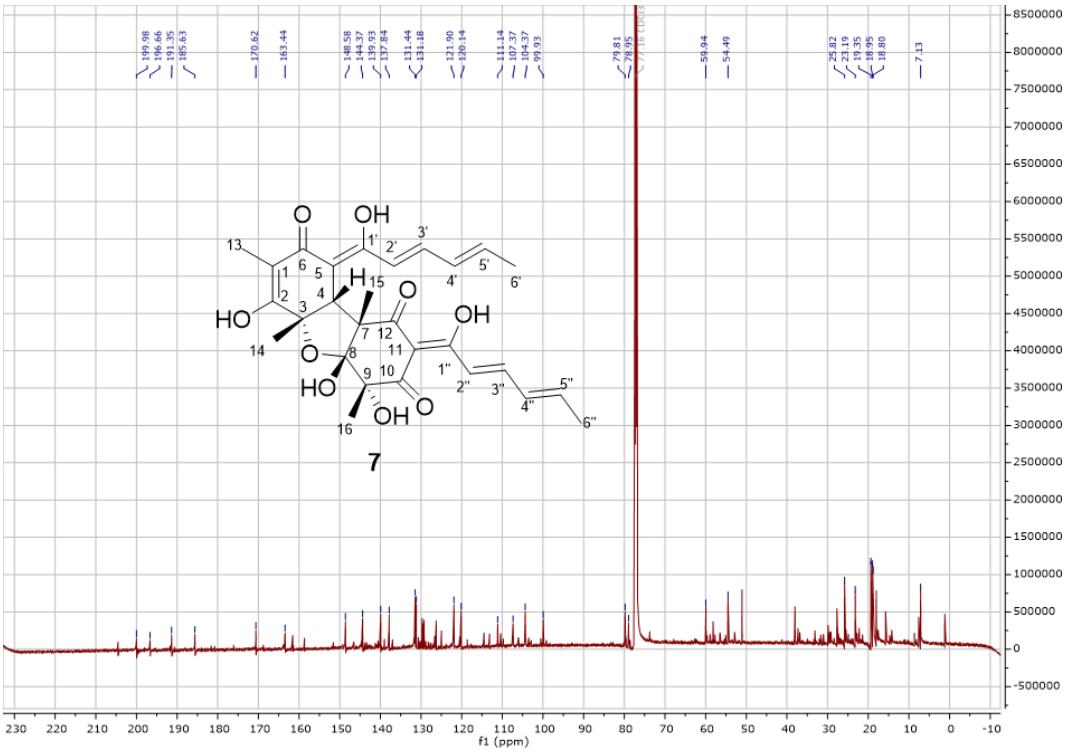

Figure S28: ^{13}C-NMR spectrum for **7a** recorded at 125 MHz in $CDCl_3$. Note: contains impurities of 2', 3'-dihydrobisvertinol **4b** or 2'', 3''-dihydrobisvertinol **4b'**.

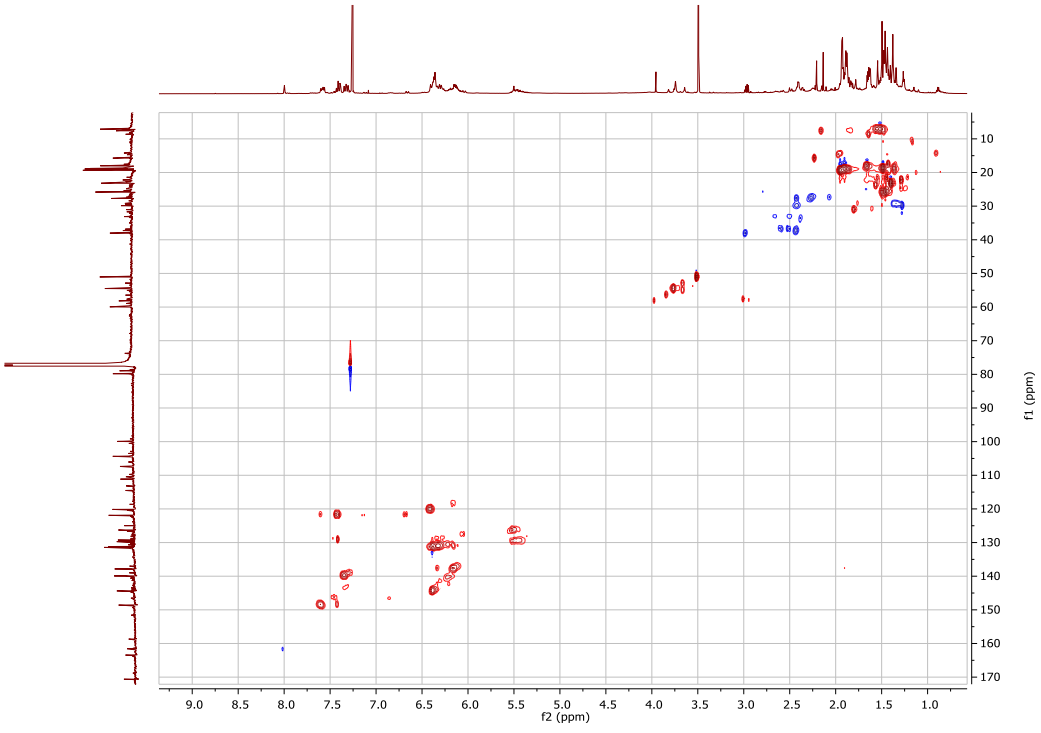

Figure S29: HSQC-spectrum for **7a** recorded in $CDCl_3$. Note: Note: contains impurities of 2', 3'-dihydrobisvertinol **4b** or 2'', 3''-dihydrobisvertinol **4b'**. Majority of impurities are displayed by the blue correlations, indicating presence of CH_2-groups of which three are present in **4b**/**4b'.**

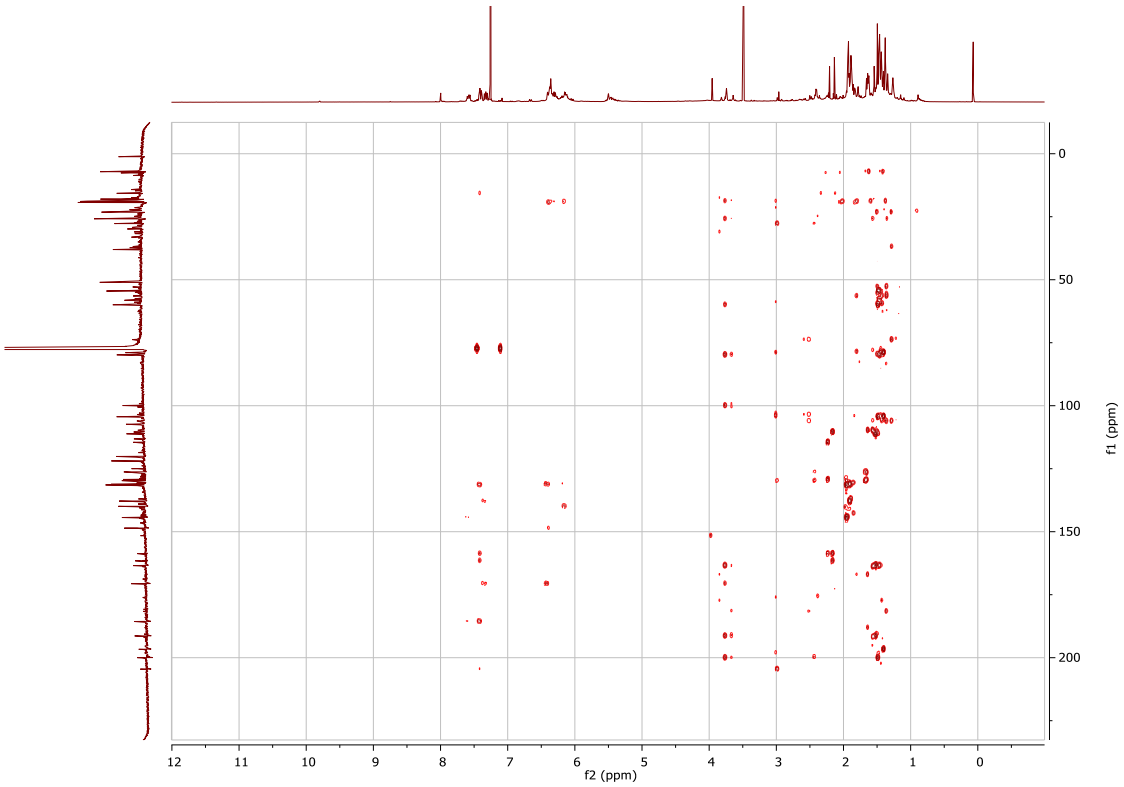

Figure S30: HMBC-spectrum for **7a** recorded in $CDCl_3$. Note: contains impurities of 2', 3'-dihydrobisvertinol **4b** or 2'', 3''-dihydrobisvertinol **4b'**. See Figure S32 for magnification of the signals characteristic for bisvertinolone **7a**.

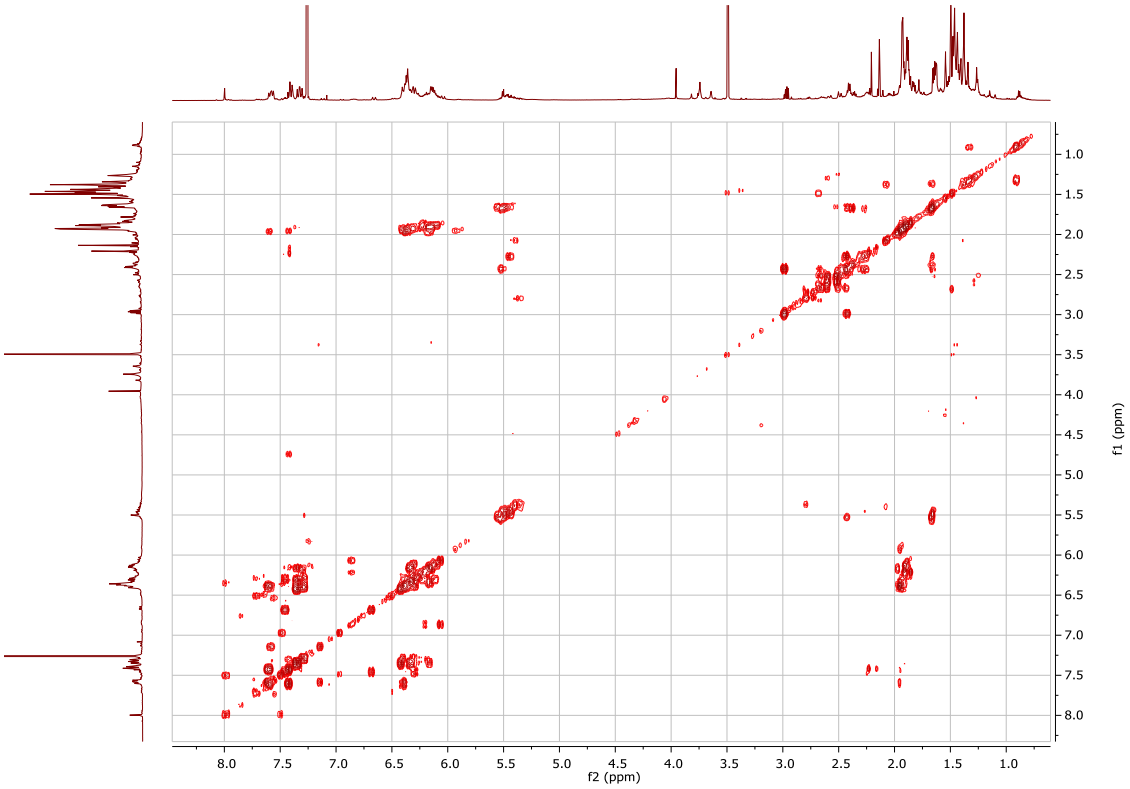

Figure S31: ^{1}H-^{1}H COSY-spectrum for **7a** recorded in $CDCl_3$. Note: contains impurities of 2', 3'-dihydrobisvertinol **4b** or 2'', 3''-dihydrobisvertinol **4b'**.

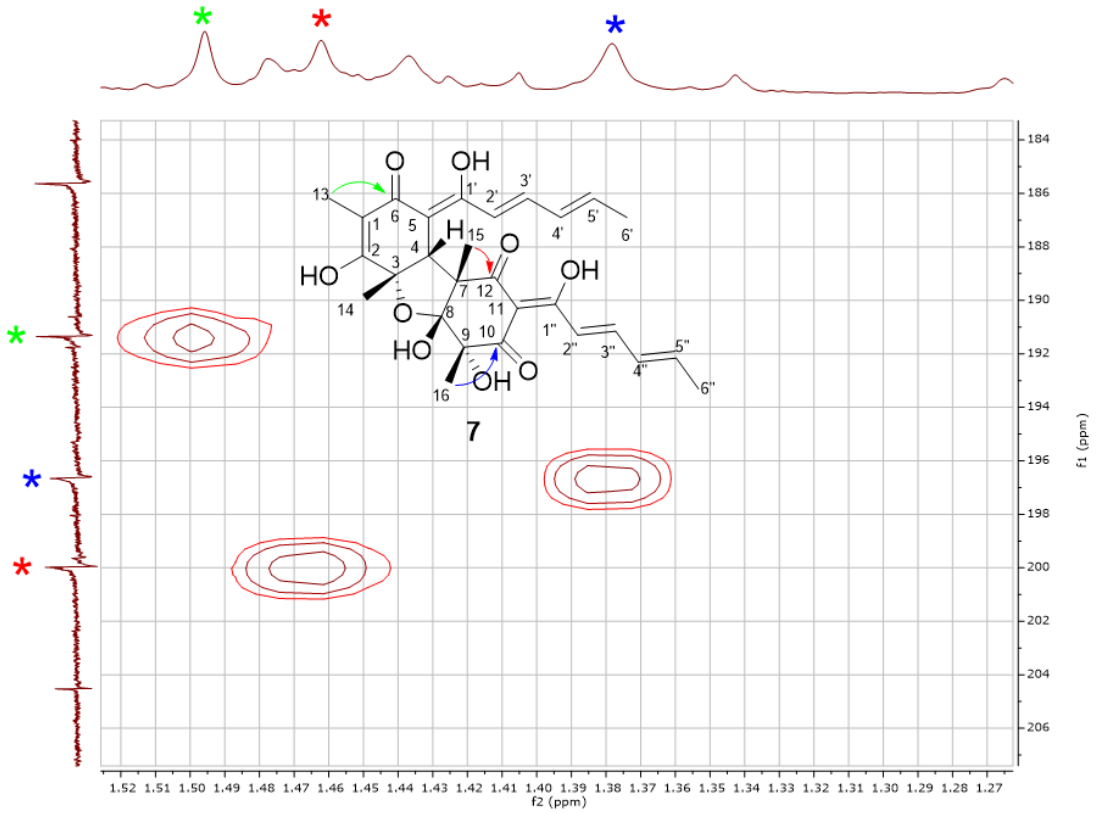

Figure S32: HMBC-correlations for **7** highlighting the C10-carbonyl group that is characteristic for bisvertinolone **7a** and distinguishes it from **4b**/**4b'**.

Compounds identified by physical properties

Compounds **6a** and **7a** were isolated and characterized within this study. Due to low titres the putative compounds **6b**, **7b** and **7b'** were proposed based on retention time, fragmentation pattern and biosynthetic considerations. Only one possible keto-enol tautomeric form is drawn. All additional compounds labelled in Figure 1 were isolated and characterized during our previous study using comprehensive NMR-analysis; except compound **4b/4b'** which was identified based on HRMS, UV-absorption and retention time (for further information the reader is referred to the respective publication).[1] Retention time, UV-absorption and fragmentation pattern of the corresponding peaks shown throughout Figure 1 are in agreement with previous data.[1] A comparison of those data between the major products of SorABCD (TrSorD) and SorABCD (PcSorD) is shown below, as well as UV-absorption and fragmentation pattern of all other compounds.

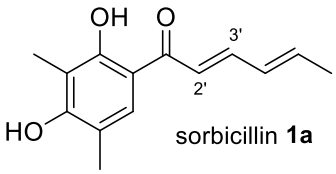

sorbicillin **1a**

Chemical Formula: $C_{14}H_{16}O_3$
Exact Mass: 232,11

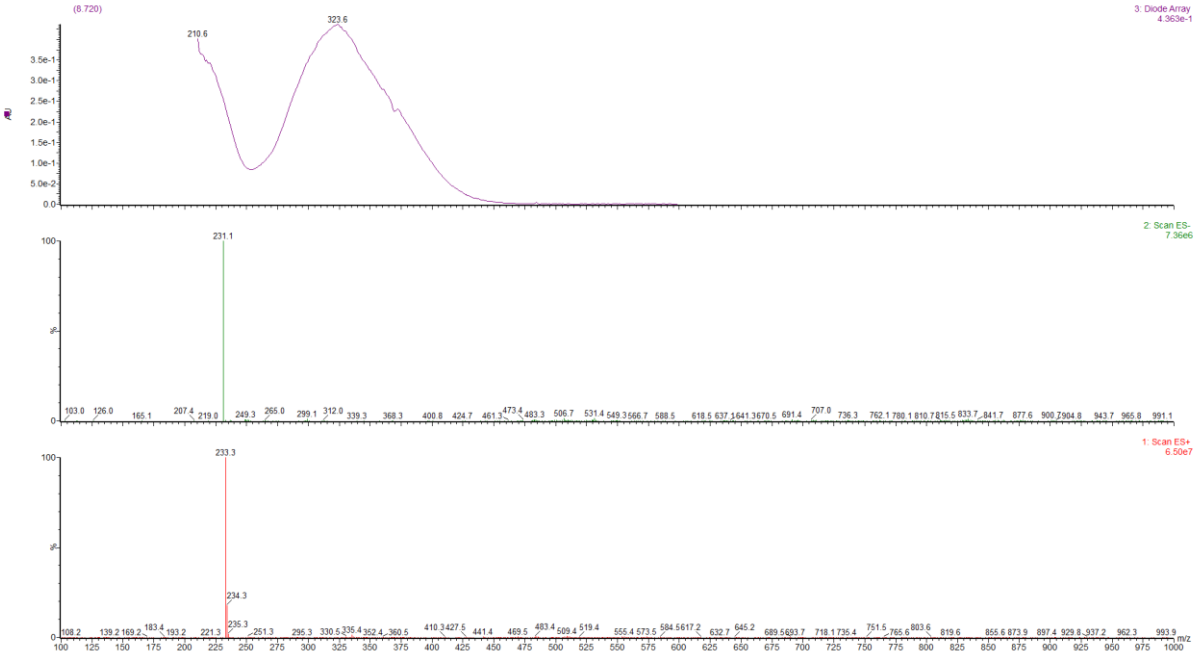

Figure S33: UV-absorption (top) and fragmentation pattern of **1a** in ES^-(middle) and ES^+ (bottom). Retention time is shown in brackets at the top left hand corner.

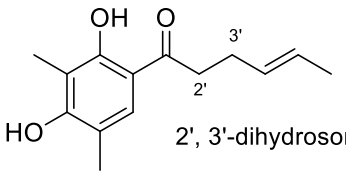

2', 3'-dihydrosorbicillin **1a**

Chemical Formula: $C_{14}H_{18}O_3$
Exact Mass: 234,13

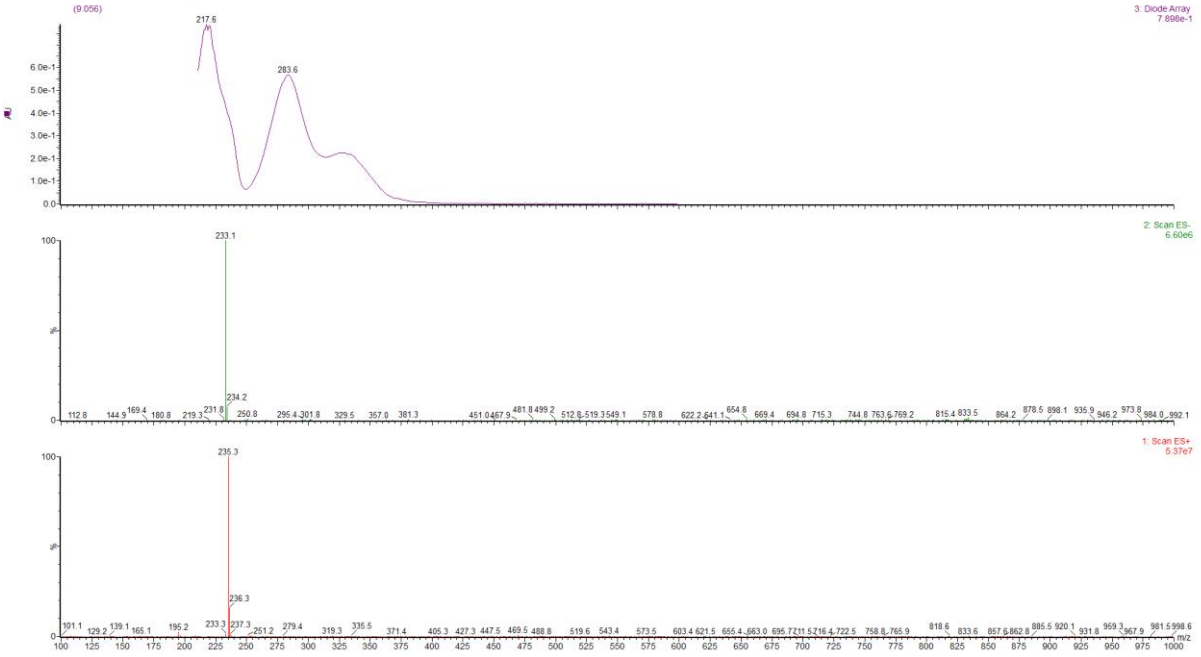

Figure S34: UV-absorption (top) and fragmentation pattern of **1b** in ES^-(middle) and ES^+ (bottom). Retention time is shown in brackets at the top left hand corner.

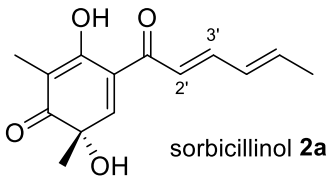

sorbicillinol **2a**

Chemical Formula: $C_{14}H_{16}O_4$
Exact Mass: 248,10

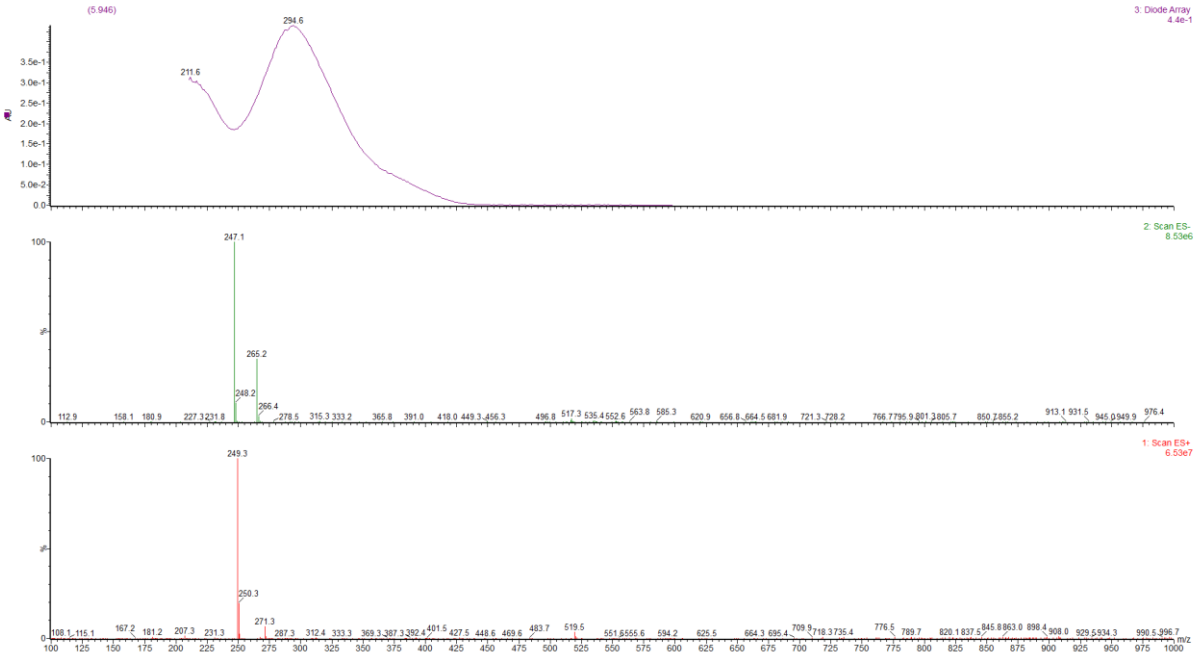

Figure S35: UV-absorption (top) and fragmentation pattern of **2a** in ES^-(middle) and ES^+ (bottom). Retention time is shown in brackets at the top left hand corner.

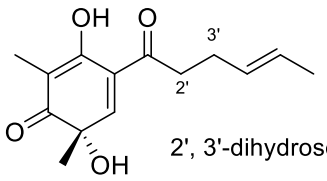

2', 3'-dihydrosorbicillinol **2b**

Chemical Formula: $C_{14}H_{18}O_4$
Exact Mass: 250,12

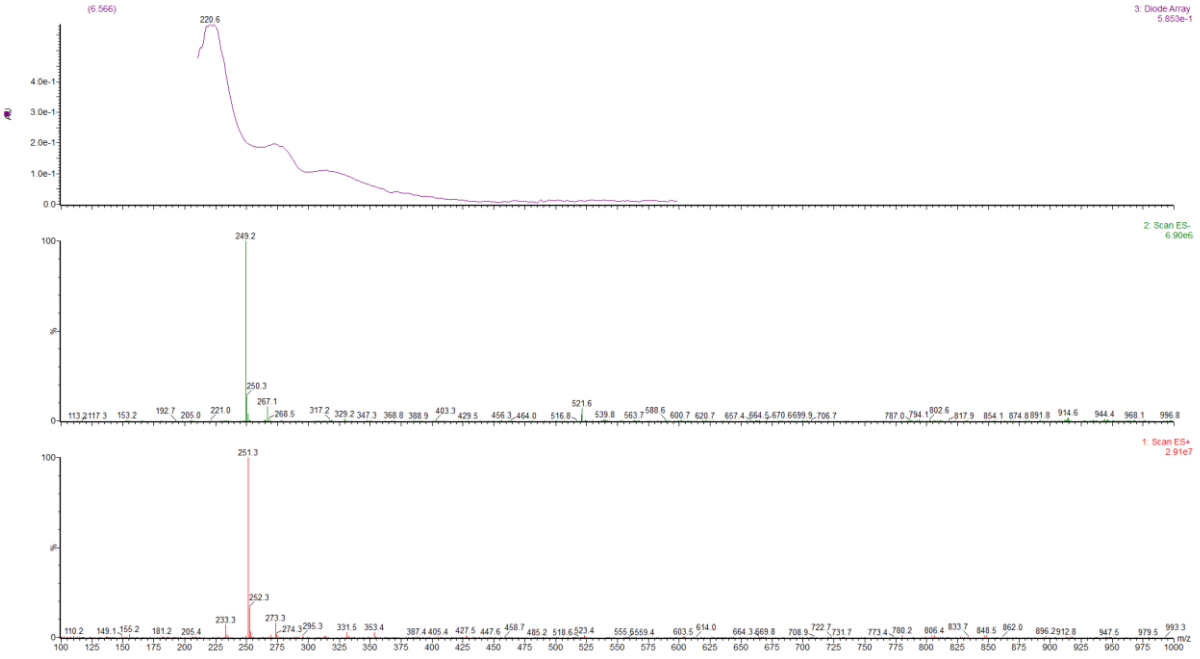

Figure S36: UV-absorption (top) and fragmentation pattern of **2b** in ES^-(middle) and ES^+ (bottom). Retention time is shown in brackets at the top left hand corner.

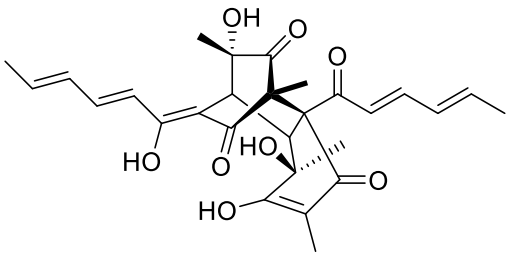

bisorbicillinol **3a**

Chemical Formula: $C_{28}H_{32}O_8$
Exact Mass: 496,21

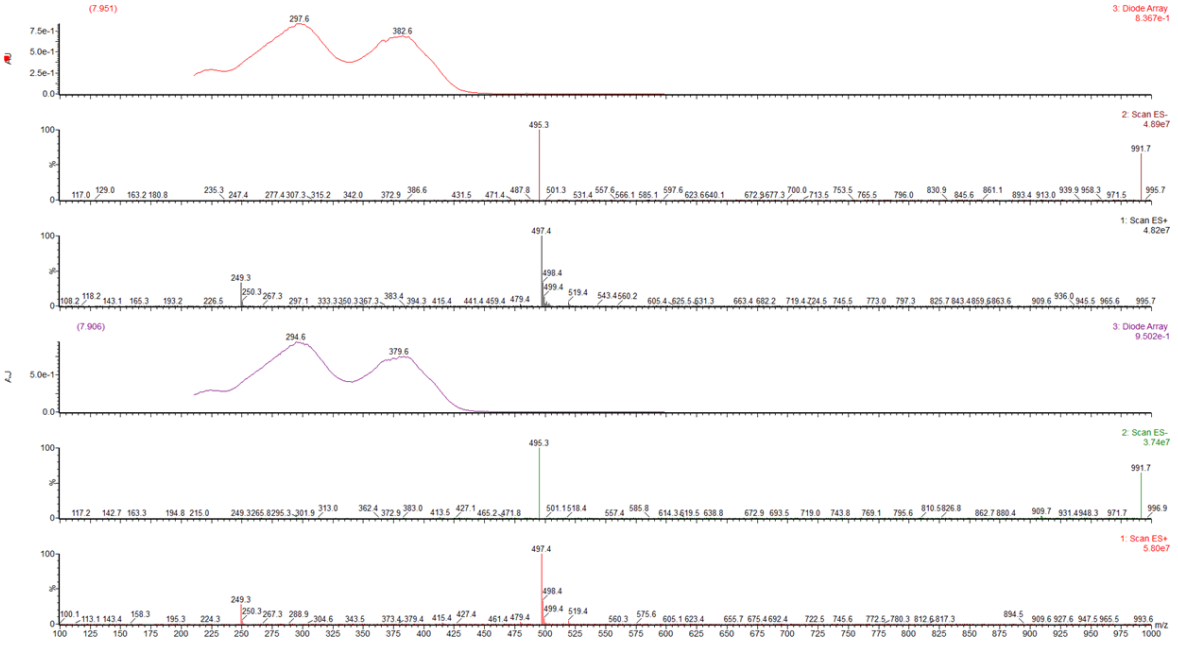

Figure S37: Comparison of UV-absorption and fragmentation pattern in ES^- and ES^+ between **3a** produced by SorABCD (TrSorD, top three chromatograms) and SorABCD (PcSorD; bottom three chromatograms). Retention time is shown in brackets at the top left hand corner.

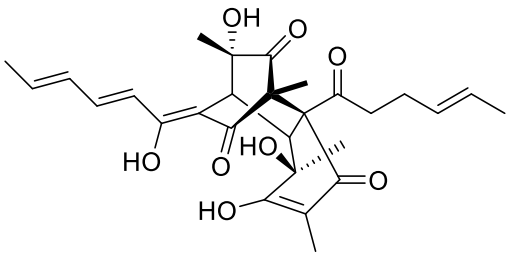

2', 3'-dihydrobisorbicillinol **3b**

Chemical Formula: $C_{28}H_{34}O_8$
Exact Mass: 498,23

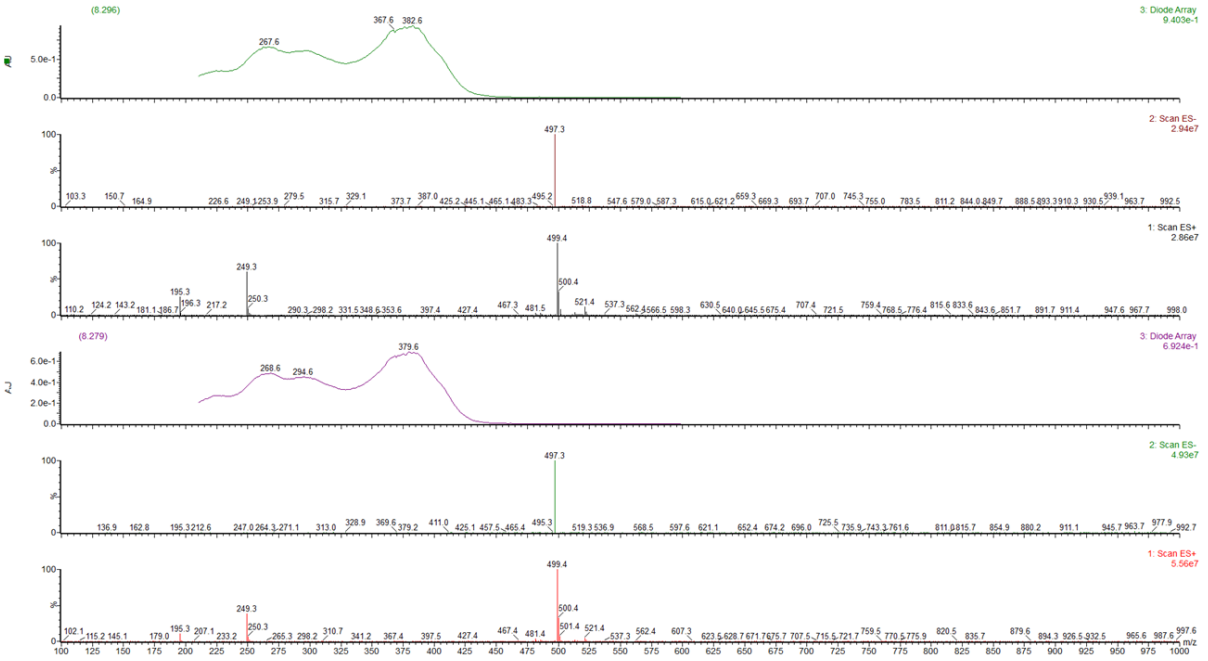

Figure S38: Comparison of UV-absorption and fragmentation pattern in ES^- and ES^+ between **3b** produced by SorABCD (TrSorD, top three chromatograms) and SorABCD (PcSorD; bottom three chromatograms). Retention time is shown in brackets at the top left hand corner.

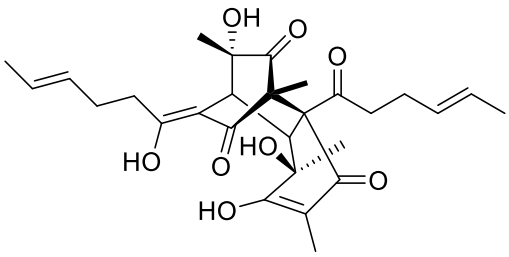

tetrahydrobisorbicillinol **3c**

Chemical Formula: $C_{28}H_{36}O_8$
Exact Mass: 500,24

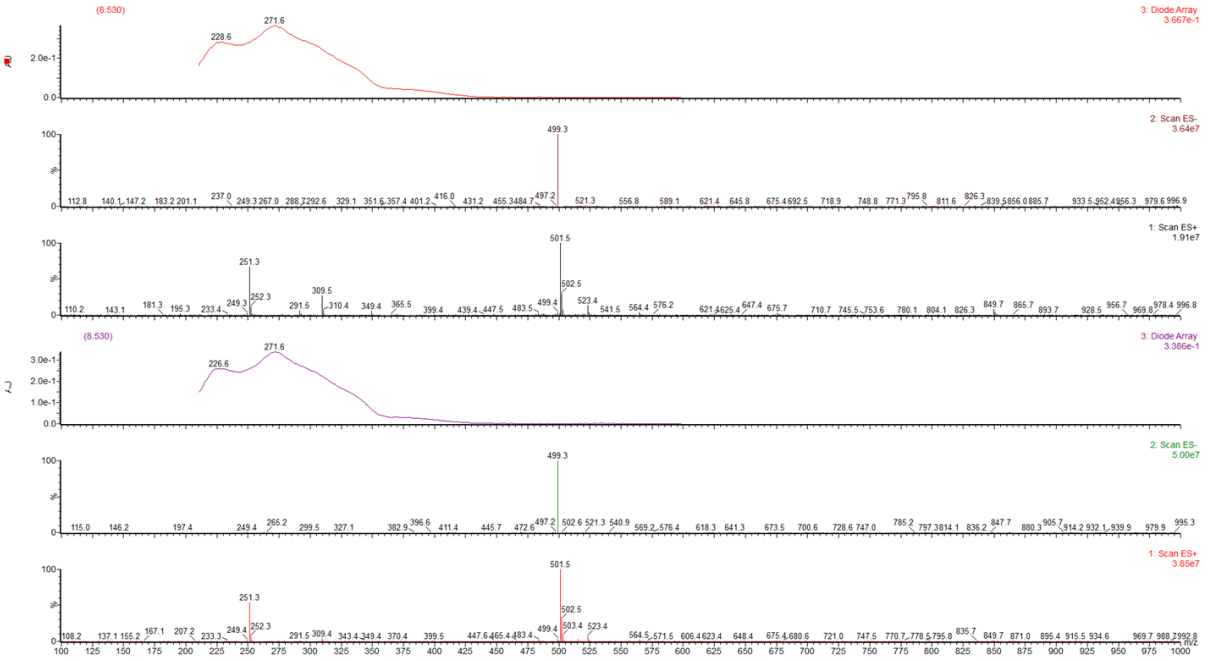

Figure S39: Comparison of UV-absorption and fragmentation pattern in ES^- and ES^+ between **3c** produced by SorABCD (TrSorD, top three chromatograms) and SorABCD (PcSorD; bottom three chromatograms). Retention time is shown in brackets at the top left hand corner.

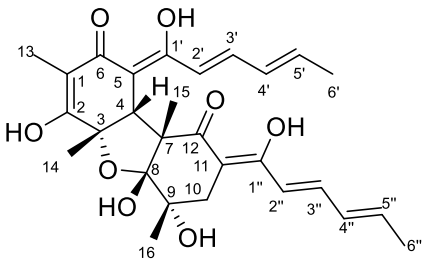

bisvertinol **4a**

Chemical Formula: $C_{28}H_{34}O_8$

Exact Mass: 498,23

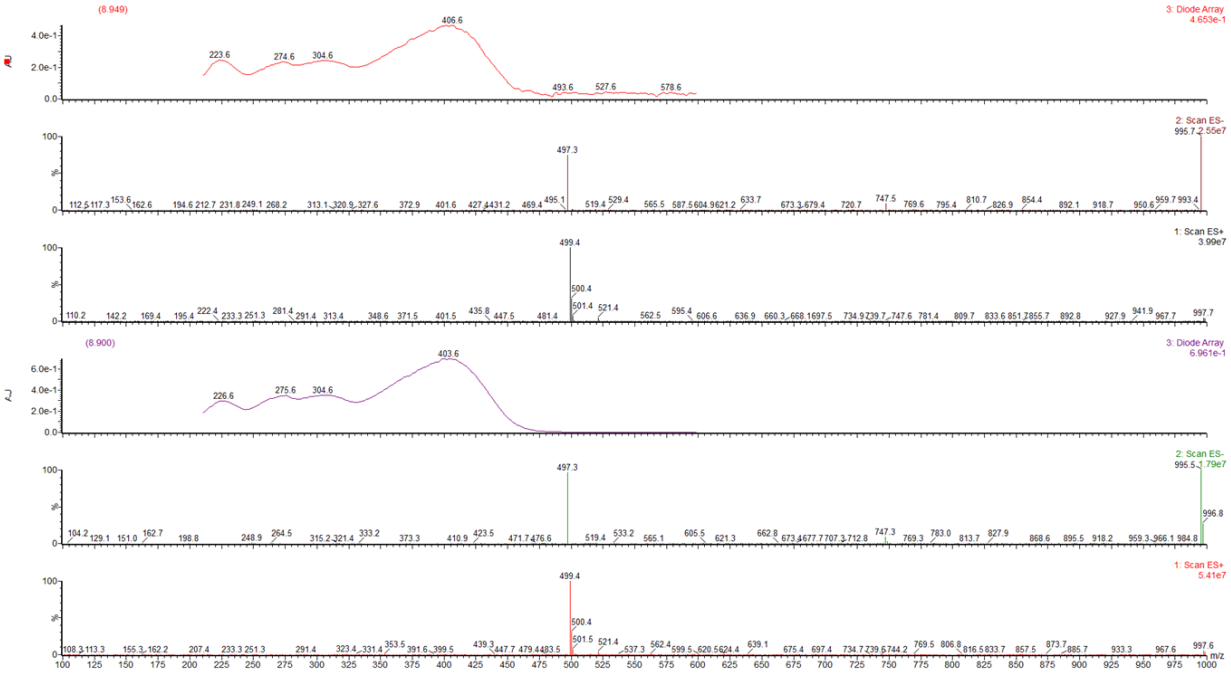

Figure S40: Comparison of UV-absorption and fragmentation pattern in ES^- and ES^+ between **4a** produced by SorABCD (TrSorD, top three chromatograms) and SorABCD (PcSorD; bottom three chromatograms). Retention time is shown in brackets at the top left hand corner.

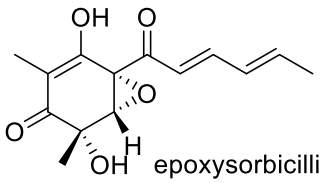

epoxysorbicillinol **5a**

Chemical Formula: $C_{14}H_{16}O_5$
Exact Mass: 264,10

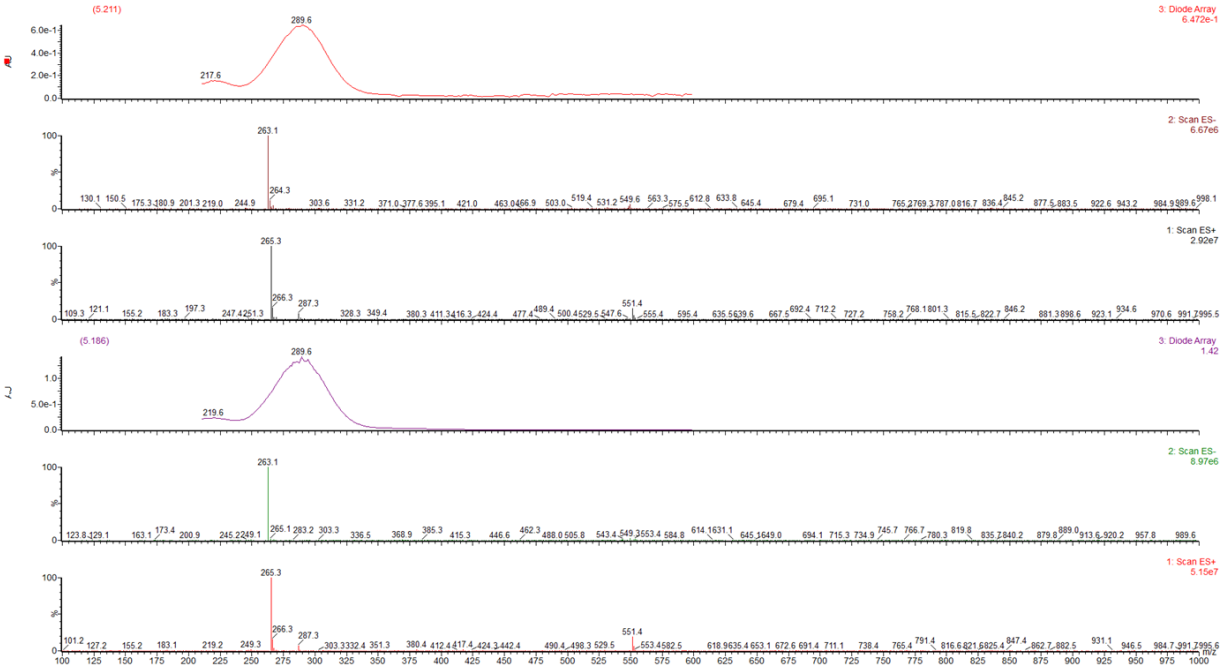

Figure S41: Comparison of UV-absorption and fragmentation pattern in ES^- and ES^+ between **5a** produced by SorABCD (TrSorD, top three chromatograms) and SorABCD (PcSorD; bottom three chromatograms). Retention time is shown in brackets at the top left hand corner.

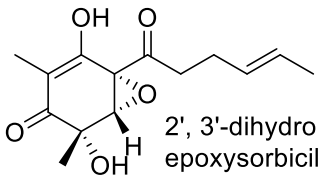

2', 3'-dihydro epoxysorbicillinol **5b**

Chemical Formula: $C_{14}H_{18}O_5$
Exact Mass: 266,12

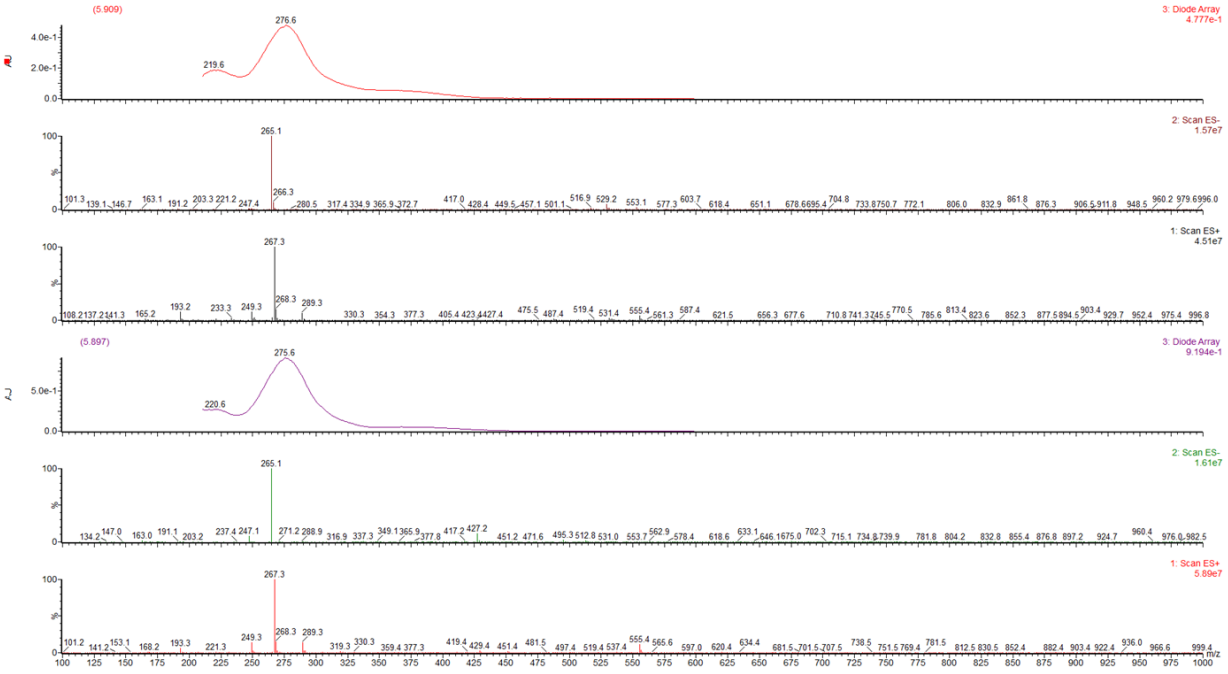

Figure S42: Comparison of UV-absorption and fragmentation pattern in ES^- and ES^+ between **5b** produced by SorABCD (TrSorD, top three chromatograms) and SorABCD (PcSorD; bottom three chromatograms). Retention time is shown in brackets at the top left hand corner.

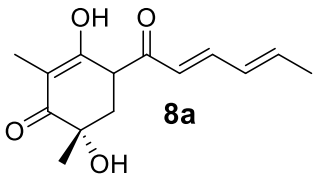

8a

Chemical Formula: $C_{14}H_{18}O_4$
Exact Mass: 250,12

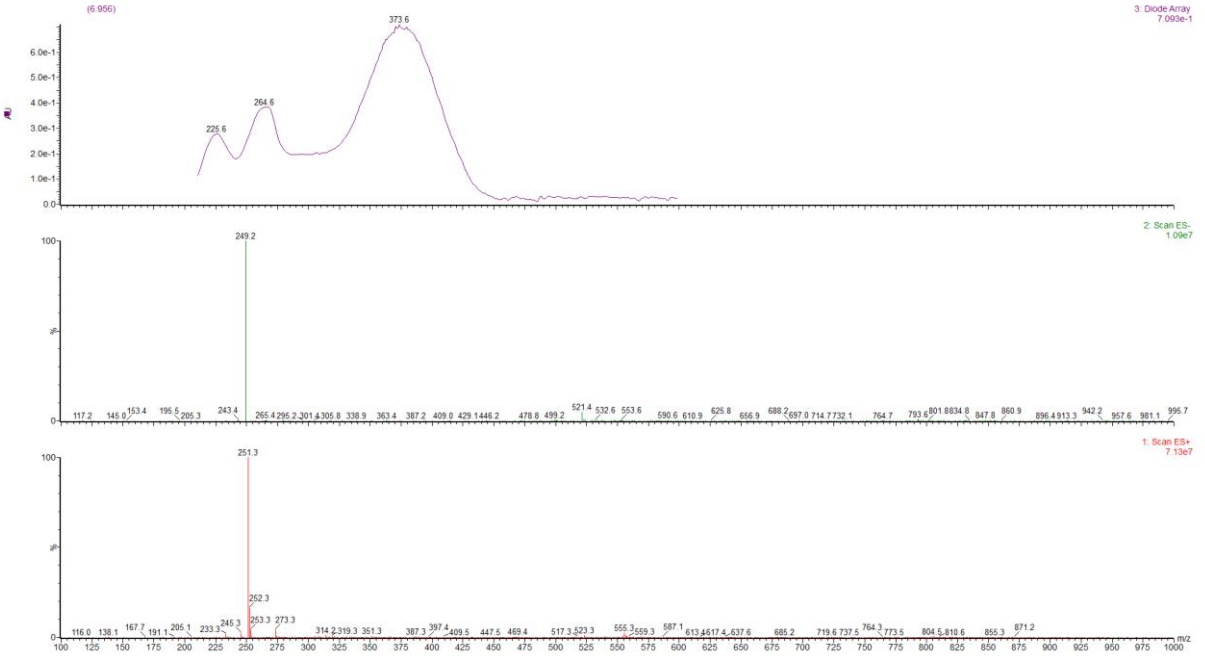

Figure S43: UV-absorption (top) and fragmentation pattern of **8a** in ES^- (middle) and ES^+ (bottom). Retention time is shown in brackets at the top left hand corner.

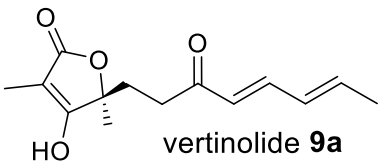

vertinolide **9a**

Chemical Formula: $C_{14}H_{18}O_4$
Exact Mass: 250,12

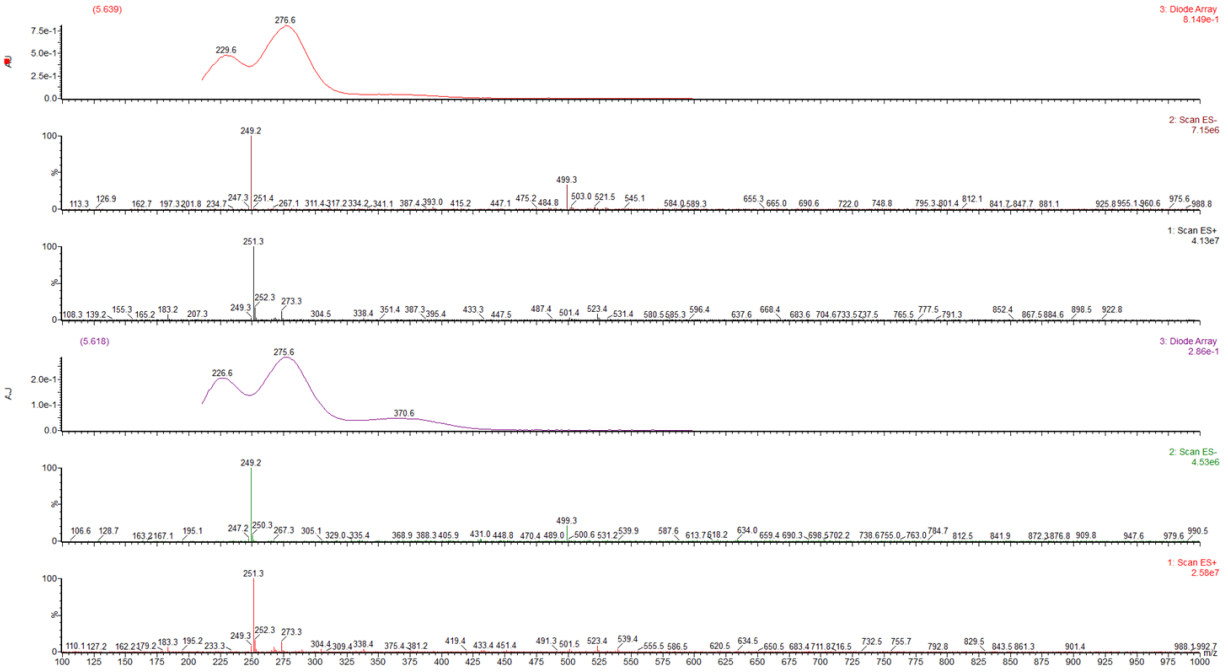

Figure S44: Comparison of UV-absorption and fragmentation pattern in ES^- and ES^+ between **9a** produced by SorABCD (TrSorD, top three chromatograms) and SorABCD (PcSorD; bottom three chromatograms). Retention time is shown in brackets at the top left hand corner.

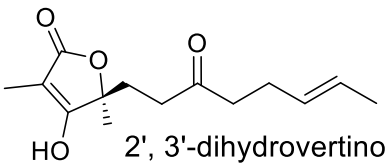

2', 3'-dihydrovertinolide **9b**

Chemical Formula: $C_{14}H_{20}O_4$
Exact Mass: 252,14

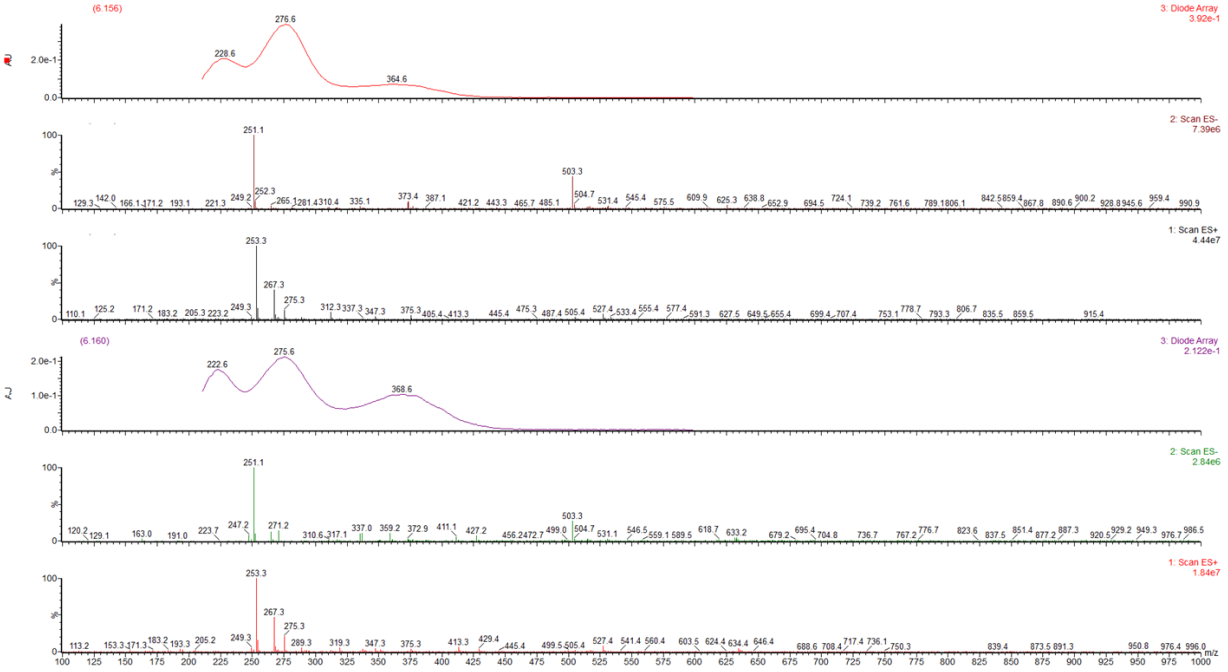

Figure S45: Comparison of UV-absorption and fragmentation pattern in ES^- and ES^+ between **9b** produced by SorABCD (TrSorD, top three chromatograms) and SorABCD (PcSorD; bottom three chromatograms). Retention time is shown in brackets at the top left hand corner.

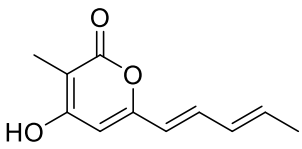

trichopyrone **10**

Chemical Formula: $C_{11}H_{12}O_3$
Exact Mass: 192,08

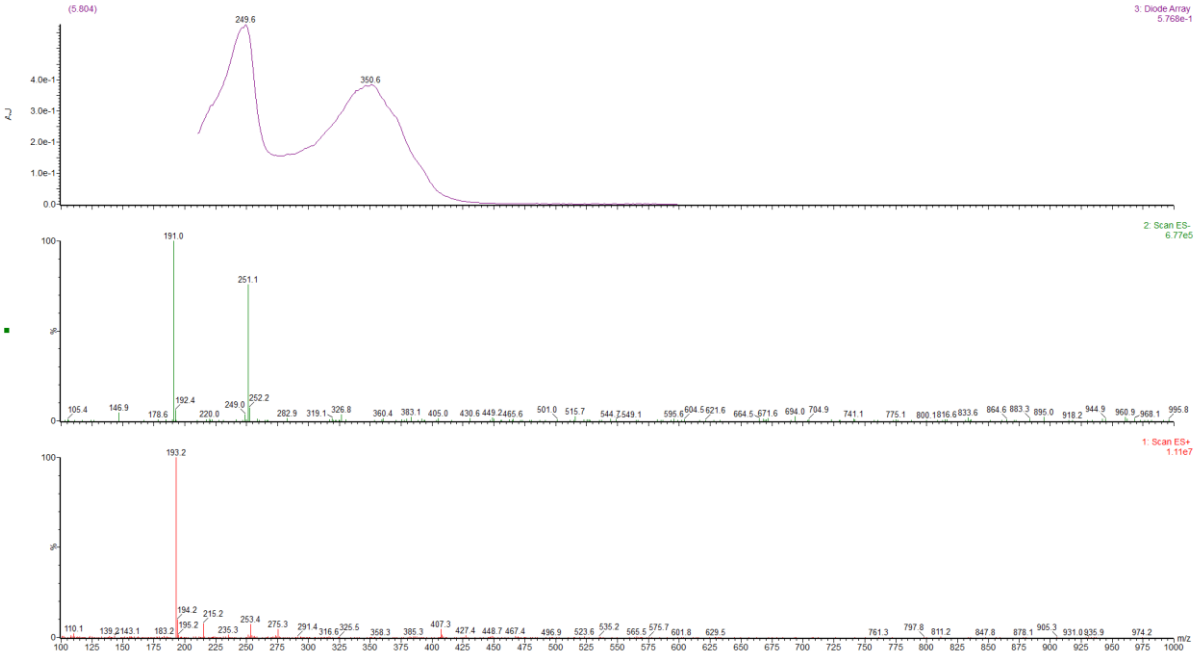

Figure S46: UV-absorption (top) and fragmentation pattern of **10** in ES^-(middle) and ES^+ (bottom). Retention time is shown in brackets at the top left hand corner.

Proposed compounds

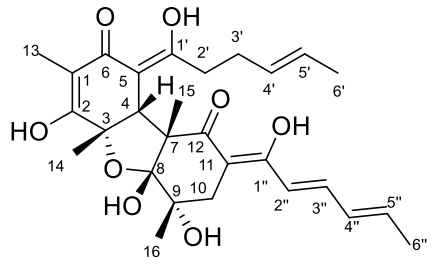

2', 3'-dihydrobisvertinol **4b**

Chemical Formula: $C_{28}H_{36}O_8$

Exact Mass: 500,24

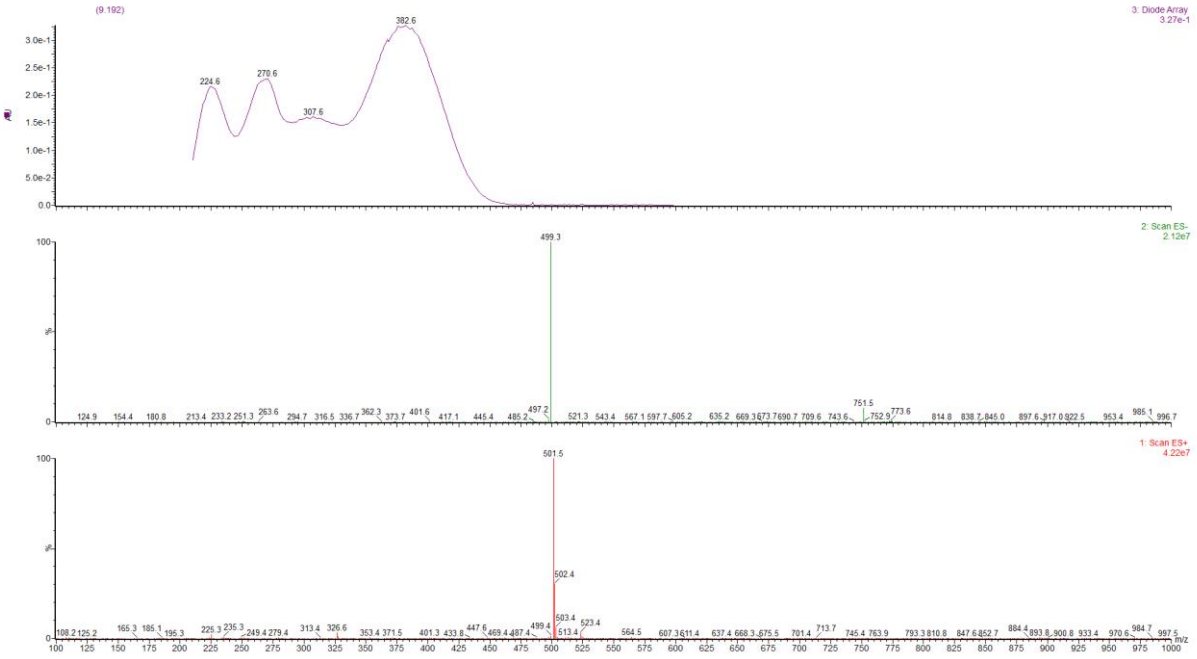

Figure S47: UV-absorption (top) and fragmentation pattern of putative **4b** in ES^-(middle) and ES^+ (bottom). Retention time is shown in brackets at the top left hand corner.

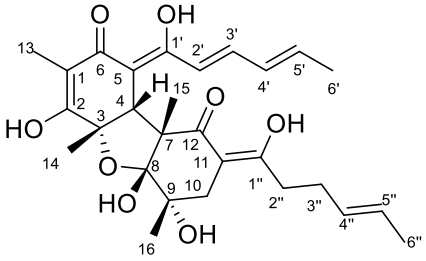

2", 3"-dihydrobisvertinol **4b'**

Chemical Formula: $C_{28}H_{36}O_8$

Exact Mass: 500,24

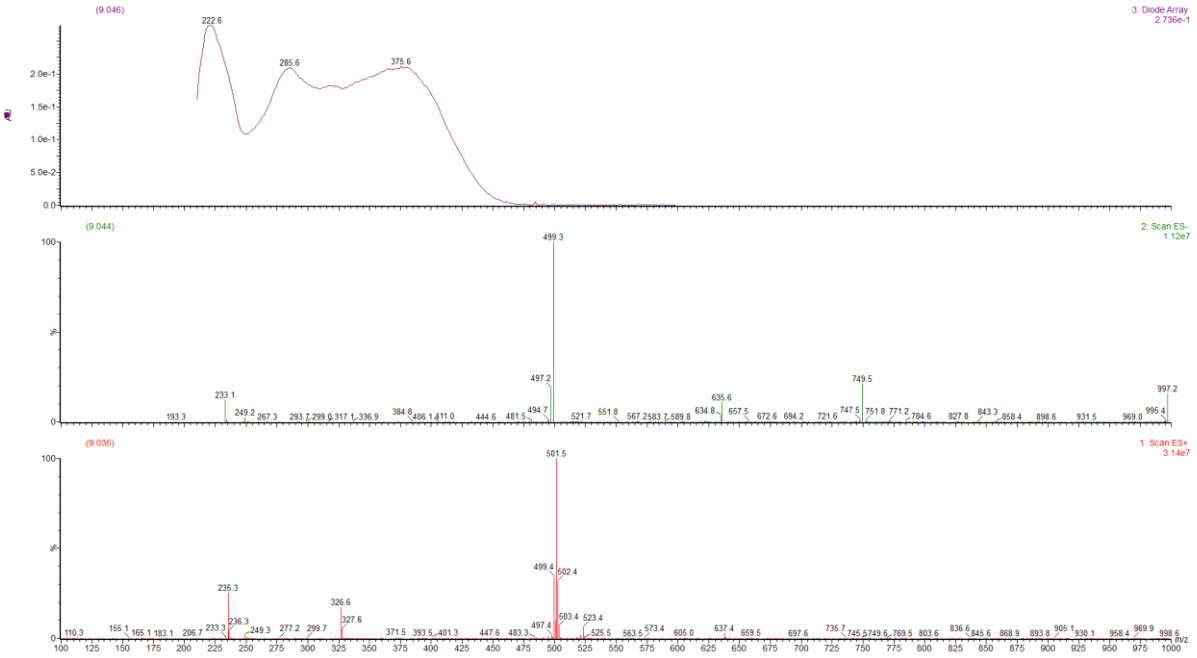

Figure S48: UV-absorption (top) and fragmentation pattern of putative **4b'** in ES^-(middle) and ES^+ (bottom). Retention time is shown in brackets at the top left hand corner. Contains impurities of **1b**.

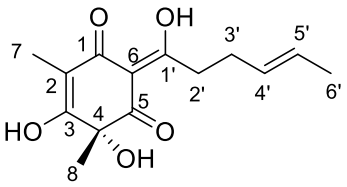

2', 3'-dihydrooxosorbicillinol **6b**

Chemical Formula: $C_{14}H_{18}O_5$
Exact Mass: 266,1154

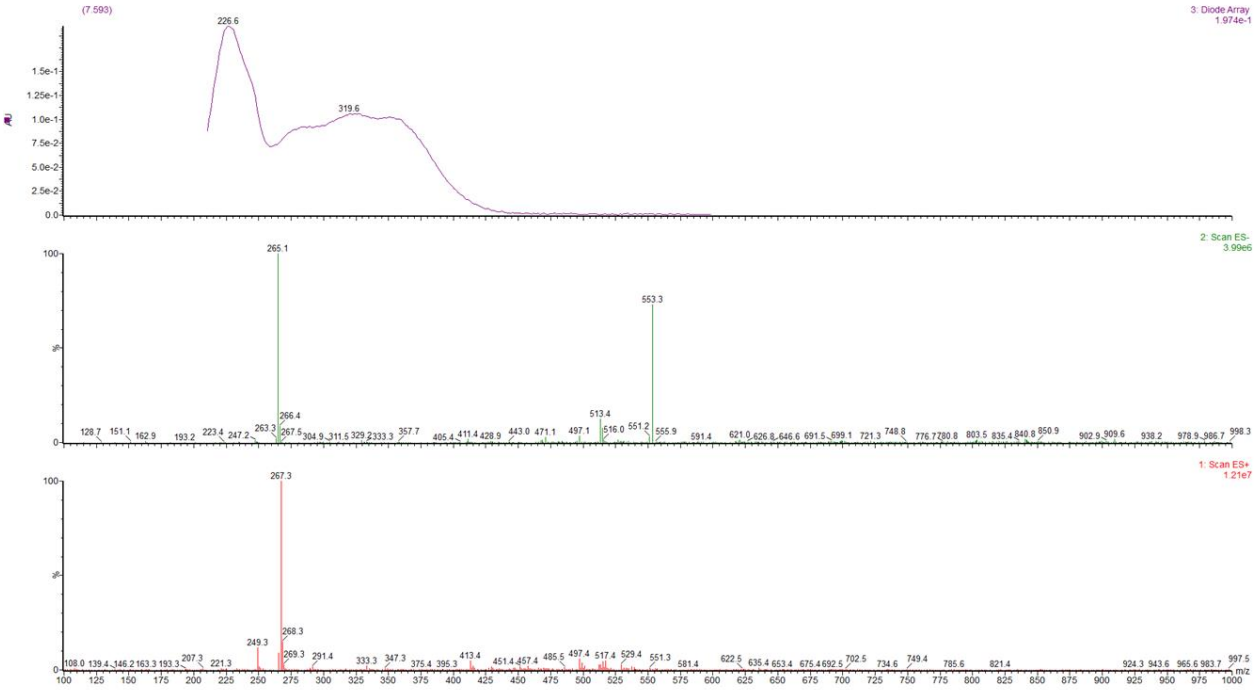

Figure S49: UV-absorption (top) and fragmentation pattern of putative **6b** in ES^-(middle) and ES^+ (bottom). Retention time is shown in brackets at the top left hand corner.

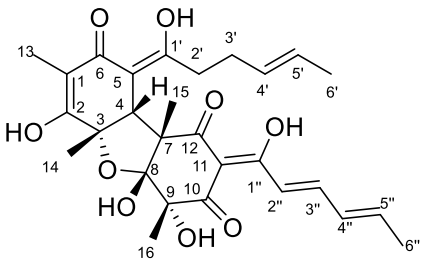

2', 3'-dihydrobisvertinolone **7b**

Chemical Formula: $C_{28}H_{34}O_9$
Exact Mass: 514,2203

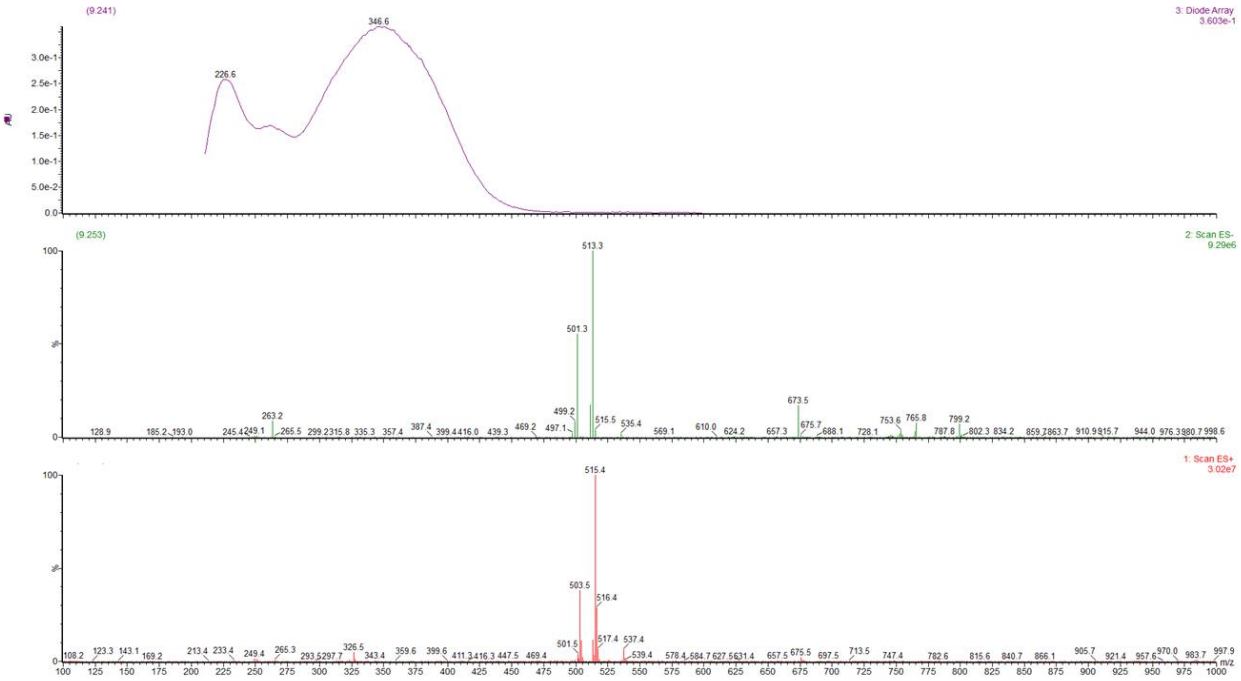

Figure S50: UV-absorption (top) and fragmentation pattern of putative **7b** in ES^-(middle) and ES^+ (bottom). Retention time is shown in brackets at the top left hand corner.

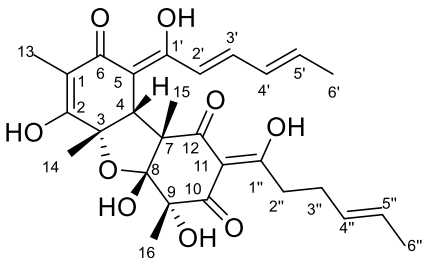

2'', 3''-dihydrobisvertinolone **7b'**

Chemical Formula: $C_{28}H_{34}O_9$

Exact Mass: 514,2203

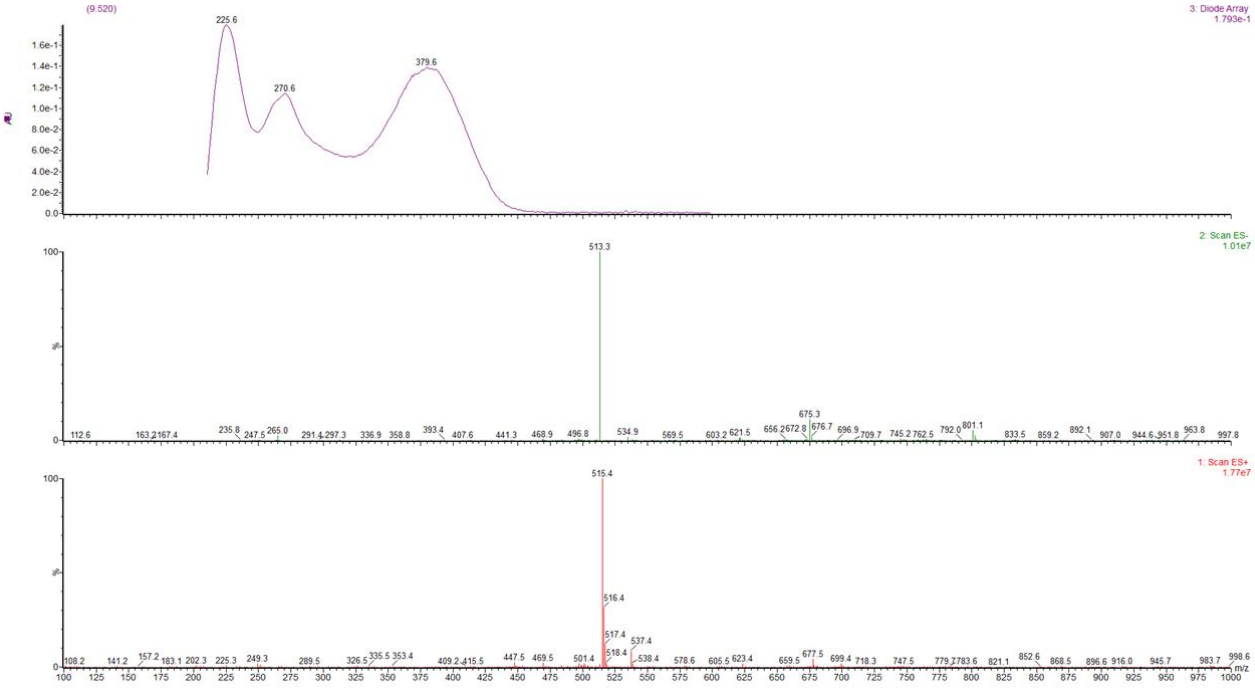

Figure S51: UV-absorption (top) and fragmentation pattern of putative **7b'** in ES^-(middle) and ES^+ (bottom). Retention time is shown in brackets at the top left hand corner.

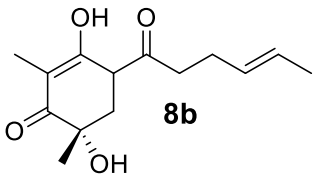

Chemical Formula: $C_{14}H_{20}O_4$
Exact Mass: 252,14

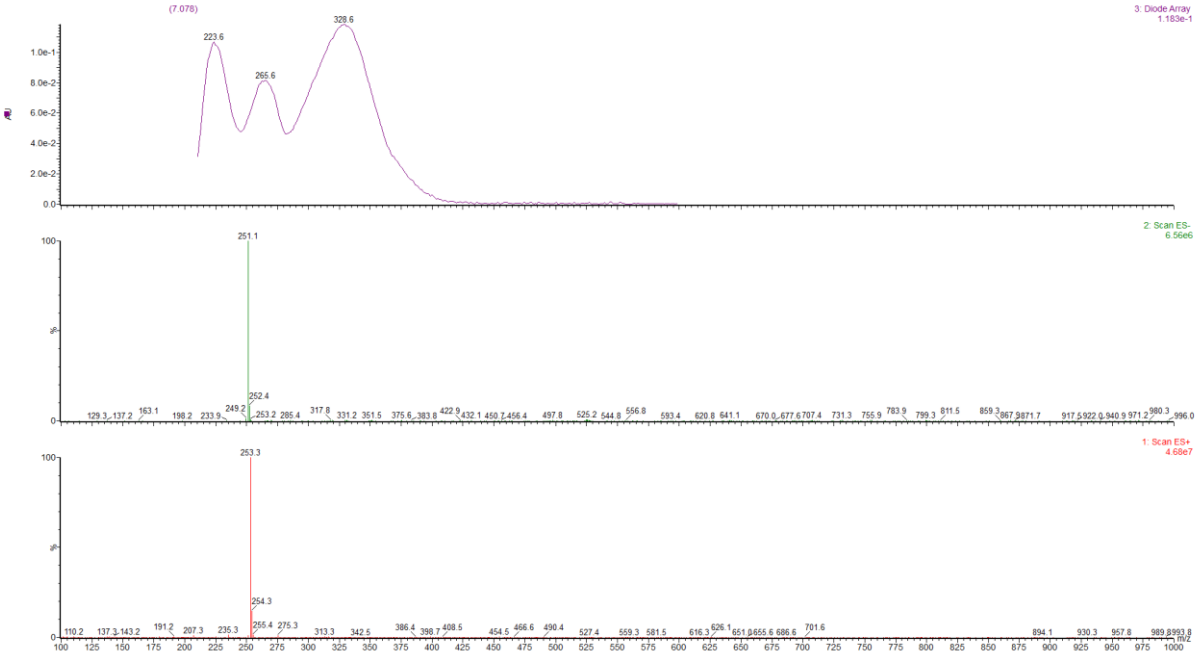

Figure S52: UV-absorption (top) and fragmentation pattern of **8b** in ES^- (middle) and ES^+ (bottom). Retention time is shown in brackets at the top left hand corner.

References

1 L. Kahlert, E. F. Bassiony, R. J. Cox and E. J. Skellam, *Angew. Chemie - Int. Ed.*, 2020, **59**, 5816–5822.

2 K. Blin, S. Shaw, K. Steinke, R. Villebro, N. Ziemert, S. Y. Lee, M. H. Medema and T. Weber, *Nucleic Acids Res.*, 2019, **47**, W81–W87.

3 V. Solovyev, P. Kosarev, I. Seledsov and D. Vorobyev, *Genome Biol.*, 2006, **7 Suppl 1**, S10.

4 T. Carver, S. R. Harris, M. Berriman, J. Parkhill and J. A. McQuillan, *Bioinformatics*, 2012, **28**, 464–469.

5 L. A. Kelley, S. Mezulis, C. M. Yates, M. N. Wass and M. J. E. Sternberg, *Nat. Protoc.*, 2015, **10**, 845–858.

6 A. R. Ferrari, H. tte J. Rozeboom, A. S. C. Vugts, M. J. Koetsier, R. Floor and M. W. Fraaije, *Molecules*, 2018, **23**, 111.

7 A. R. Ferrari, H. J. Rozeboom, J. M. Dobruchowska, S. S. Van Leeuwen, A. S. C. Vugts, M. J. Koetsier, J. Visser, M. W. Fraaije and G. Hart, *J. Biol. Chem.*, 2016, **291**, 23709–23718.

8 C. Derntl, F. Guzmán-Chávez, T. M. Mello-de-Sousa, H. J. Busse, A. J. M. Driessen, R. L. Mach and A. R. Mach-Aigner, *Front. Microbiol.*, 2017, **8**, 2037.

9 M. J. Cao, T. Zhu, J. T. Liu, L. Ouyang, F. Yang and H. W. Lin, *Nat. Prod. Res.*, 2019, 1–7.

10 R. Andrade, W. A. Ayer and L. S. Trifonov, *Can. J. Chem.*, 1996, **74**, 371–379.

11 W. Liu, Q. Gu, W. Zhu, C. Cui and G. Fan, *J. Antibiot. (Tokyo).*, 2005, **58**, 621–624.

12 K. Washida, N. Abe, Y. Sugiyama and A. Hirota, *Biosci. Biotechnol. Biochem.*, 2007, **71**, 1052–1057.

13 G. Bringmann, G. Lang, T. A. M. Gulder, H. Tsuruta, J. Mühlbacher, K. Maksimenka, S. Steffens, K. Schaumann, R. Stöhr, J. Wiese, J. F. Imhoff, S. Perović-Ottstadt, O. Boreiko and W. E. G. Müller, *Tetrahedron*, 2005, **61**, 7252–7265.

14 L. Du, T. Zhu, Y. Li, S. Cai, B. Zhao and Q. Gu, *Chem. Pharm. Bull.*, 2009, **57**, 220–223.

15 R. P. Maskey, I. Grün-Wollny and H. Laatsch, *J. Nat. Prod.*, 2005, **68**, 865–870.

16 G. Bringmann, G. Lang, T. Bruhn, K. Schäffler, S. Steffens, R. Schmaljohann, J. Wiese and J. F. Imhoff, *Tetrahedron*, 2010, **66**, 9894–9901.

17 O. Salo, F. Guzmán-Chávez, M. I. Ries, P. P. Lankhorst, R. A. L. Bovenberg, R. J. Vreeken and A. J. M. Driessen, *Appl. Environ. Microbiol.*, 2016, **82**, 3971–3978.

18 F. Guzmán-Chávez, O. Salo, Y. Nygård, P. P. Lankhorst, R. A. L. Bovenberg and A. J. M. Driessen, *Microb. Biotechnol.*, 2017, **10**, 958–968.

19 M. Sato, J. E. Dander, C. Sato, Y. S. Hung, S. S. Gao, M. C. Tang, L. Hang, J. M. Winter, N. K. Garg, K. Watanabe and Y. Tang, *J. Am. Chem. Soc.*, 2017, **139**, 5317–5320.

20 K. Neumann, A. Abdel-Lateff, A. D. Wright, S. Kehraus, A. Krick and G. M. König, *European J. Org. Chem.*, 2007, **2007**, 2268–2275.

21 Q. Gao, J. E. Leet, S. T. Thomas, J. A. Matson and D. P. Bancroft, *J. Nat. Prod.*, 1995, **58**, 1817–1821.

22 J. Y. Ueda, J. Hashimoto, S. Inaba, M. Takagi and K. Shin-Ya, *J. Antibiot. (Tokyo).*, 2010, **63**, 203–205.

23 N. Abe, T. Murata, K. Yamamoto and A. Hirota, *Tetrahedron Lett.*, 1999, **40**, 5203–5206.

24 N. Abe, T. Murata and A. Hirota, *Biosci. Biotechnol. Biochem.*, 1998, **62**, 2120–2126.

25 T. Komoda and M. Nishikawa, *Biosci. Biotechnol. Biochem.*, 2012, **76**, 1404–1406.

26 G. Wohlfahrt, S. Witt, J. Hendle, D. Schomburg, H. M. Kalisz and H. J. Hecht, *Acta Crystallogr. Sect. D Biol. Crystallogr.*, 1999, **55**, 969–977.

27 M. G. Madej, H. R. Nasiri, N. S. Hilgendorff, H. Schwalbe and C. R. D. Lancaster, *EMBO J.*, 2006, **25**, 4963–4970.

28 Y. Nakajima, I. Miyahara, K. Hirotsu, Y. Nishina, K. Shiga, C. Setoyama, H. Tamaoki and R. Miura, *J. Biochem.*, 2002, **131**, 365–374.

29 P. Pongpamorn, P. Watthaisong, P. Pimviriyakul, A. Jaruwat, N. Lawan, P. Chitnumsub and P. Chaiyen, *ChemBioChem*, 2019, **20**, 3020–3031.

30 D. Leys, J. Basran and N. S. Scrutton, *EMBO J.*, 2003, **22**, 4038–4048.

31 P. Trickey, M. A. Wagner, M. S. Jorns and F. S. Mathews, *Structure*, 1999, **7**, 331–345.

32 A. Mattevi, M. W. Fraaije, A. Mozzarelli, L. Olivi, A. Coda and W. J. H. Van Berkel, *Structure*, 1997, **5**, 907–920.

33 Q. T. Nguyen, G. de Gonzalo, C. Binda, A. Rioz-Martínez, A. Mattevi and M. W. Fraaije, *ChemBioChem*, 2016, **17**, 1359–1366.

34 J. Jin, H. Mazon, R. H. H. Van Den Heuvel, D. B. Janssen and M. W. Fraaije, *FEBS J.*, 2007, **274**, 2311–2321.

35 L. M. Cunane, Z. W. Chen, W. S. McIntire and F. S. Mathews, *Biochemistry*, 2005, **44**, 2963–2973.

36 Y. Lindqvist, *J. Mol. Biol.*, 1989, **209**, 151–166.

37 S. Montersino, R. Orru, A. Barendregt, A. H. Westphal, E. Van Duijn, A. Mattevi and W. J. H. Van Berkel, *J. Biol. Chem.*, 2013, **288**, 26235–26245.

38 E. Malito, A. Coda, K. D. Bilyeu, M. W. Fraaije and A. Mattevi, *J. Mol. Biol.*, 2004, **341**, 1237–1249.

39 F. Forneris, D. P. H. M. Heuts, M. Delvecchio, S. Rovida, M. W. Fraaije and A. Mattevi, *Biochemistry*, 2008, **47**, 978–985.

40 J. W. A. Koetter and G. E. Schulz, *J. Mol. Biol.*, 2005, **352**, 418–428.

41 R. Teufel, A. Miyanaga, Q. Michaudel, F. Stull, G. Louie, J. P. Noel, P. S. Baran, B. Palfey and B. S. Moore, *Nature*, 2013, **503**, 552–556.

42 A. Sultana, I. Alexeev, I. Kursula, P. Mäntsälä, J. Niemi and G. Schneider, *Acta Crystallogr. Sect. D Biol. Crystallogr.*, 2007, **63**, 149–159.

43 Y. C. Liu, Y. S. Li, S. Y. Lyu, L. J. Hsu, Y. H. Chen, Y. T. Huang, H. C. Chan, C. J. Huang, G. H. Chen, C. C. Chou, M. D. Tsai and T. L. Li, *Nat. Chem. Biol.*, 2011, **7**, 304–309.

44 C. H. Huang, W. L. Lai, M. H. Lee, C. J. Chen, A. Vasella, Y. C. Tsai and S. H. Liaw, *J. Biol. Chem.*, 2005, **280**, 38831–38838.

45 D. P. H. M. Heuts, D. B. Janssen and M. W. Fraaije, *FEBS Lett.*, 2007, **581**, 4905–4909.

46 B. Daniel, T. Pavkov-Keller, B. Steiner, A. Dordic, A. Gutmann, B. Nidetzky, C. W. Sensen, E. Van Der Graaff, S. Wallner, K. Gruber and P. Macheroux, *J. Biol. Chem.*, 2015, **290**, 18770–18781.

47 S. Wallner, A. Winkler, S. Riedl, C. Dully, S. Horvath, K. Gruber and P. MacHeroux, *Biochemistry*, 2012, **51**, 6139–6147.

48 K. A. K. Pahirulzaman, K. Williams and C. M. Lazarus, in *Methods in Enzymology*, Academic Press, 2012, vol. 517, pp. 241–260.

49 N. Abe, T. Arakawa and A. Hirota, *Chem. Commun.*, 2002, **2**, 204–205.

50 A. Sib and T. A. M. Gulder, *Angew. Chemie - Int. Ed.*, 2018, **57**, 14650–14653.